SC-R-64-147

Sandia Corporation

REPRINT

THE PROPAGATION OF TRANSIENT ELECTROMAGNETIC FIELDS INTO A CAVITY FORMED BY TWO IMPERFECTLY CONDUCTING SHEETS

by

C W Harrison, Jr, M L Houston,
R W P King, and Tai Tsun Wu

APRIL 1964

SC-R-64-147

SANDIA CORPORATION MONOGRAPH

THE PROPAGATION OF TRANSIENT ELECTROMAGNETIC FIELDS INTO A CAVITY FORMED BY TWO IMPERFECTLY CONDUCTING SHEETS

by

C. W. Harrison, Jr., and M. L. Houston,
Sandia Corporation,

R. W. P. King, and Tai Tsun Wu,
Harvard University

April 1964

SUMMARY

In this paper steady-state formulas are developed for the ratio of the resultant electromagnetic field in the screened space formed by dual, infinite, homogeneous metal plates to the incident field, and from these transfer functions the time history of the field in the cavity is computed for Gaussian-shaped input fields.

ACKNOWLEDGMENTS

The authors are indebted to Dr. H. J. Schmitt and Mr. C. S. Williams, Jr. for suggestions.

The problem was programmed for the Sandia Laboratory CDC-1604 computer by Mr. E. Aronson.

TABLE OF CONTENTS

LIST OF ILLUSTRATIONS

THE PROPAGATION OF TRANSIENT ELECTROMAGNETIC FIELDS INTO A CAVITY FORMED BY TWO IMPERFECTLY CONDUCTING SHEETS

1. Introduction

The purpose of this paper is to investigate the propagation of an electromagnetic pulse through a shield consisting of two infinite identical parallel imperfectly conducting metal sheets. Specifically, the time histories of the electric and magnetic fields are calculated within the cavity, and on the far side of the dual-plate shield, when the incident electric or magnetic field is a plane wave with an amplitude distribution in the shape of a Gaussian pulse.

A problem of current interest is the determination of the fields in the interior of imperfectly conducting metallic containers which are exposed to the strong electromagnetic signals emanating from nuclear explosions. Such containers always have finite dimensions along which resonant currents may be excited at certain characteristic frequencies. Before a study is made of shielding by such finite containers it is advantageous to investigate the physically unrealizable but analytically much simpler problem of shielding by a cavity formed by two parallel infinite metal plates when a plane electromagnetic disturbance in the form of a pulse is incident from one side. Although the results obtained with such an infinite shield cannot be expected to yield quantitative information on the magnitude of the field in a finite shield when resonances occur, the general significance of partial reflection and transmission on the one hand, and of skin effect and attenuation on the other should be the same in infinite and finite shields.

The electric-field shielding ratio, under steady-state or transient conditions, is defined to be the ratio of the peak field at a selected point within the shield to the amplitude of the incident field, that is, of the field that would exist at the same point with the shield removed. The shielding ratio for the magnetic field is defined in the same way. A different shielding ratio is obtained if it is defined in terms of the field inside and outside the shield since the field outside the shield is the resultant of the incident and backscattered fields.

In the first part of the paper the steady-state transfer functions for use in a Fourier integral are developed in general terms with no restrictions on the frequency other than those implied in the assumption that the shielding plates are quite highly conducting so that at all relevant frequencies the inequality $\sigma \gg 2\pi f\epsilon_o$ is satisfied where σ is the conductivity of the metal shields. The thickness of the plates used in the shields and the distance between them is arbitrary with respect to the wavelength of the incident radiation.

In the latter part of the paper the use of the Fourier integral to obtain the time histories of the electric and magnetic fields at selected points throughout the shield is explained briefly, and an appropriate form is developed for evaluation by a high-speed digital computer. An estimate is also obtained of the decay time in the cavity of a delta-function electromagnetic pulse incident on the cavity.

In conclusion, the numerical results are presented graphically and discussed.

2. Fundamentals

Maxwell's equations in free space for a periodically varying source* are

$$\nabla \times H = j2\pi f\epsilon_o E \tag{1}$$

$$\nabla \times E = -j2\pi f\mu_o H. \tag{2}$$

In a homogeneous region of conductivity $\sigma >> 2\pi f\epsilon_o$, dielectric constant ϵ_o and permeability μ_o, the equation corresponding to (1) is

$$\nabla \times H = \sigma E, \tag{3}$$

where E and H are the vector electric and magnetic field phasors, respectively. f is the frequency in cycles/sec, $\epsilon_o = 8.85 \times 10^{-12}$ farads/m, and $\mu_o = 4\pi \times 10^{-7}$ henry/m. σ is measured in mhos/m. It should be noted that (2) applies both in free space and in the conducting medium if it is nonmagnetic.

---

*The assumed time dependence of the electric vector is $Ee^{j2\pi ft}$ where $E = E(x, y, z; f)$. Since $E = \hat{x}E_x + \hat{y}E_y + \hat{z}E_z$, the time dependence of the y-component is

$$E_y e^{j2\pi ft} = E_y(x, y, z; f)\, e^{j2\pi ft}.$$

From a solution for the harmonic dependence, a solution may be obtained for a more general time dependence by means of the Fourier representation

$$e_y(x, y, z; t) = \int_{-\infty}^{\infty} E_y(x, y, z; f) e^{j2\pi ft}\, df.$$

Note that lower-case letters, such as $e_y(x, y, z; t)$, are used for time functions, and upper-case letters, such as $E_y(x, y, z; f)$, for frequency functions. The two are, of course, Fourier pairs.

In the particular shielding problem involving plane waves discussed in this paper the following notation is used: $E_y(x, y, z; f) = E_y(x; f)$, $e_y(x, y, z; t) = e_y(x; t)$, $H_z(x, y, z; f) = H_z(x; f)$, $h_z(x, y, z; t) = h_z(x; t)$ For a plane wave traveling in the positive x-direction the instantaneous electric and magnetic fields are related by $e_y(x; t) = \zeta_o h_z(x; t)$ where $\zeta_o = \sqrt{\mu_o/\epsilon_o} = 120\pi$ ohms.

If $E = \hat{y}E_y$, and the plane-wave field is propagating in the x-direction, $H = \hat{z}H_z$. Then (1)-(3) become

$$E_y = \frac{j}{2\pi f\epsilon_o} \frac{\partial H_z}{\partial x} \tag{4}$$

$$H_z = \frac{j}{2\pi f\mu_o} \frac{\partial E_y}{\partial x} \tag{5}$$

$$E_y = -\frac{1}{\sigma} \frac{\partial H_z}{\partial x} . \tag{6}$$

The wave equations satisfied by E_y in free space and in the conducting region are easily obtained from Maxwell's Equations (1)-(3). These are

$$\frac{\partial^2 E_y}{\partial x^2} + \beta^2 E_y = 0 \tag{7}$$

and

$$\frac{\partial^2 E_y}{\partial x^2} + k^2 E_y = 0. \tag{8}$$

In (7),

$$\beta = 2\pi f\sqrt{\mu_o\epsilon_o} = \frac{2\pi}{\lambda} \tag{9}$$

where λ is the wavelength in air, and in (8),

$$k = \sqrt{\pi f\mu_o\sigma}(1 - j). \tag{10}$$

3. Derivation of the Steady-State Shielding Transfer Functions for the Electric and Magnetic Fields

(a) Preliminary Remarks

Figure 1 illustrates a dual-plate shield. The cavity formed by the identical, infinite, imperfectly conducting, homogeneous parallel plates is of width 2b. The total width of the shield is 2a. Hence the width of each plate is $d = a - b$. The cavity, metal plates, and outside space are designated regions 1, 2, and 3, respectively. The origin of a Cartesian coordinate system is at the middle of the cavity. The y and z axes are parallel to the plates. The direction of propagation of the incident electromagnetic field is in the positive x-direction. It is assumed that the electric field has only a y-component and the magnetic field a z-component. The radiation impinges on the shield at $x = -a$, where a standing wave is developed, and emerges from the shield at $x = a$ as a traveling wave. $E_o(f)$ and $E_R(f)$ are the incident and reflected electric fields, respectively, and $E_T(a;f)$ represents the field emerging from the

shield. The notation $E_i(-b;f)$, $E_i(0;f)$, and $E_i(b;f)$ is used to represent the electric fields inside the cavity at the left side, middle, and right side, respectively. The corresponding terminology for the H-field is $H_o(f)$, $H_R(f)$, $H_T(a;f)$, $H_i(-b;f)$, $H_i(0;f)$, and $H_i(b;f)$. The incident field is $E_y(x;f) = E_o(f)e^{-j\beta x}$; $H_z(x;f) = H_o(f)e^{-j\beta x}$ where $H_o(f) = E_o(f)/\zeta_o$.

The various transfer functions needed to solve this shielding problem, of which $E_i(-b;f)/E_o(f)$ and $H_i(0;f)/H_o(f)$ are typical, may be found by solving the boundary value problem represented by Figure 1 directly. In carrying out the work, nine constants must be introduced (one of which is assumed to be known). An equivalent procedure is to employ the method of symmetrical phase components. In Figure 2, the problem to be solved, (c), is split into symmetrical and antisymmetrical parts, (a) and (b), respectively. In this drawing the directions of propagation and polarizations of all electric fields are shown. When the identical shields (a) and (b) are superimposed, (c) is obtained. Superposition cancels all fields on the plate at $x = a$ except the transmitted field $E_T(a;f)$. On the plate at $x = -a$ the resultant field is $E_t(-a;f) = E_o(-a;f) + E_R(-a;f)$. Note that only five constants (one of which is known) need be introduced to solve the symmetrical problem (a), and the same number to solve the antisymmetrical problem (b).

(b) The Shielding Problem for Symmetrical Electric Field Excitation

The problem of shielding for symmetrical excitation (with the electric field even and the magnetic field odd in x) is illustrated in Figure 2a. The plane waves $\frac{1}{2}E_o(f)e^{j\beta x}$ and $\frac{1}{2}E_o(f)e^{-j\beta x}$ travel from both sides toward the shield. The solutions of wave equations (7) and (8), valid in the regions designated by the subscripts 1, 2, and 3, are

$$E^s_{y_1}(x;f) = C_1(e^{j\beta x} + e^{-j\beta x}); \quad H^s_{z_1}(x;f) = -\frac{C_1}{\zeta_o}\left(e^{j\beta x} - e^{-j\beta x}\right) \tag{11}$$

$$E^s_{y_2}(x;f) = C_2e^{jkx} + C_3e^{-jkx}; \quad H^s_{z_2}(x;f) = -\frac{1}{\zeta_o}\left(C_2e^{j\beta x} - C_3e^{-j\beta x}\right) \tag{12}$$

$$E^s_{y_3}(x;f) = C_4e^{j\beta x} + C_5e^{-j\beta x}; \quad H^s_{z_3}(x;f) = -\frac{1}{\zeta_o}\left(C_4e^{j\beta x} - C_5e^{-j\beta x}\right), \tag{13}$$

where (11) satisfies (7) and meets the required symmetry conditions $E^s_{y_1}(x;f) = E^s_{y_1}(-x;f)$, and $H^s_{z_1}(x;f) = -H^s_{z_1}(-x;f)$.

The next step is to impose the boundary conditions characteristic of the problem. For this purpose consider the region $0 \le x \le a$ where the incident field is $\frac{1}{2}E_o(f)e^{j\beta x}$.

Continuity of the electric field at $x = b$ and $x = a$ leads to the equations

$$C_1(e^{j\beta b} + e^{-j\beta b}) = C_2e^{jkb} + C_3e^{-jkb} \tag{14}$$

$$C_2e^{jka} + C_3e^{-jka} = C_4e^{j\beta a} + C_5e^{-j\beta a}, \tag{15}$$

where now $C_4 = \frac{1}{2} E_o(f)$. Continuity of the magnetic field at $x = b$ and $x = a$ leads to the following additional equations:

$$\zeta C_1\left(e^{j\beta b} - e^{-j\beta b}\right) = \zeta_o\left(C_2 e^{jkb} - C_3 e^{-jkb}\right) \tag{16}$$

$$\zeta_o\left(C_2 e^{jka} - C_3 e^{-jka}\right) = \zeta\left(C_4 e^{j\beta a} - C_5 e^{-j\beta a}\right) \tag{17}$$

where

$$\zeta = \sqrt{\frac{\pi f \mu_o}{\sigma}}\,(1 + j) \tag{18}$$

and

$$\zeta_o = \sqrt{\frac{\mu_o}{\epsilon_o}} \approx 120\pi \text{ ohms.} \tag{19}$$

Note that

$$k\zeta = \beta\zeta_o = \omega\mu_o,\ k/\zeta = -j\sigma \tag{20}$$

for nonmagnetic conductors.

Let the ratio of the amplitude of the field in the shielded region 1 to the field incident from region 3 with $x > a$ be denoted by

$$S_1(f) = \frac{C_1}{C_4} = \frac{2C_1}{E_o(f)}\,. \tag{21}$$

This ratio is found from (14)-(17) to be:

$$S_1(f) = \frac{\zeta\zeta_o(\cos\beta a + j\sin\beta a)}{\zeta\zeta_o(\cos\beta b + j\sin\beta b)\cos kd + j\left(\zeta_o^2\cos\beta b + j\zeta^2\sin\beta b\right)\sin kd}\,. \tag{22}$$

From (21) and (11), the electric field in the shielded region when symmetrically excited is

$$E^s_{y_1}(x;f) = E_o(f)S_1(f)\cos\beta x. \tag{23}$$

The associated magnetic field is obtained from the application of (5) to (23). Thus

$$H^s_{z_1}(x;f) = -jH_o(f)S_1(f)\sin\beta x \tag{24}$$

where

$$H_o(f) = \frac{E_o(f)}{\zeta_o}\,. \tag{25}$$

It follows that in the middle of the cavity $x = 0$, $H^s_{z_1}(0;f) = 0$ and $E^s_{y_1}(0;f)$ is a maximum. Here the superscripts s refer to symmetrical electric and antisymmetrical magnetic field excitation.

(c) The Shielding Problem for Antisymmetrical Electric Field Excitation

The problem of shielding for antisymmetrical excitation (with an odd electric and an even magnetic field) is illustrated in Figure 2b. The plane waves $-\frac{1}{2}E_o(f)e^{j\beta x}$ and $\frac{1}{2}E_o(f)e^{-j\beta x}$ travel from the two sides toward the shield. The solutions of wave equations (7) and (8) and the associated magnetic field as obtained with (5) are:

$$E^a_{y_1}(x;f) = C'_1\left(e^{j\beta x} - e^{-j\beta x}\right); \quad H^a_{z_1} = -\frac{C'_1}{\zeta_o}\left(e^{j\beta x} + e^{-j\beta x}\right) \tag{26}$$

$$E^a_{y_2}(x;f) = C'_2e^{jkx} + C'_3e^{-jkx}; \quad H^a_{z_2} = -\frac{1}{\zeta_o}\left(C'_2e^{j\beta x} - C'_3e^{-j\beta x}\right) \tag{27}$$

$$E^a_{y_3}(x;f) = C'_4e^{j\beta x} + C'_5e^{-j\beta x}; \quad H^a_{z_3} = -\frac{1}{\zeta_o}\left(C'_4e^{j\beta x} - C'_5e^{-j\beta x}\right). \tag{28}$$

Note that (26) satisfies (7) and meets the required symmetry conditions $E^a_{y_1}(x;f) = -E^a_{y_1}(-x;f)$ and $H^a_{z_1}(x;f) = H^a_{z_1}(-x;f)$. The application of the boundary conditions, as in the symmetrical problem, leads to the following equations:

$$C'_1\left(e^{j\beta b} - e^{-j\beta b}\right) = C'_2e^{jkb} + C'_3e^{-jkb} \tag{29}$$

$$C'_2e^{jka} + C'_3e^{-jka} = C'_4e^{j\beta a} + C'_5e^{-j\beta a} \tag{30}$$

$$\zeta C'_1\left(e^{j\beta b} + e^{-j\beta b}\right) = \zeta_o\left(C'_2e^{jkb} - C'_3e^{-jkb}\right) \tag{31}$$

$$\zeta_o\left(C'_2e^{jka} - C'_3e^{-jka}\right) = \zeta\left(C'_4e^{j\beta a} - C'_5e^{-j\beta a}\right), \tag{32}$$

where now $C'_4 = -\frac{1}{2}E_o(f)$. The ratio of the amplitude of the electric field in the shielded region 1 to the incident field from region 3 with $x > a$ is

$$A_1(f) = \frac{C'_1}{C'_4} = -\frac{2C'_1}{E_o(f)} \tag{33}$$

where the negative sign before $E_o(f)/2$ in (33) takes account of the fact that the antisymmetrical incident electric field from region 3 is reversed in phase from that in the symmetrical case.

The value of $A_1(f)$ is

$$A_1(f) = \frac{\zeta\zeta_o(\cos\beta a + j\sin\beta a)}{\zeta\zeta_o(\cos\beta b + j\sin\beta b)\cos kd + j\left(\zeta^2\cos\beta b + j\zeta_o^2\sin\beta b\right)\sin kd}. \tag{34}$$

From (33) and (26) the antisymmetrical electric field in the shielded region 1 is

$$E^a_{y_1}(x;f) = -jE_o(f)A_1(f)\sin\beta x. \tag{35}$$

The associated magnetic field is obtained from (35) with (5). Thus,

$$H^{a}_{z_1}(x;f) = H_o(f)A_1(f)\cos \beta x. \tag{36}$$

Evidently with antisymmetrical electric-field excitation the electric field is zero and the magnetic field has a maximum at $x = 0$.

(d) Total Electric and Magnetic Fields in the Cavity

The complete electric field in the cavity due to a single incident electric field $E_o(f)e^{-j\beta x}$, Figure 2c, is the sum of (23) and (35). Thus

$$E_i(x;f) = E^{s}_{y_1}(x;f) + E^{a}_{y_1}(x;f) = E_o(f)\left[S_1(f)\cos \beta x - jA_1(f)\sin \beta x\right]. \tag{37}$$

Graphs of the ratio $E_i(x;f)/E_o(f)$ in decibels* are shown in Figures 3a, b, c for the three points $x = -b$, 0, and b. Note that $E_i(0;f)/E_o(f) = S_1(f)$. The associated magnetic field in the cavity is the sum of (24) and (36). It is

$$H_i(x;f) = H^{s}_{z_1}(x;f) + H^{a}_{z_1}(x;f) = H_o(f)\left[A_1(f)\cos \beta x - jS_1(f)\sin \beta x\right] \tag{38}$$

where as before, $H_o(f) = E_o(f)/\zeta_o$. The ratio $H_i(0;f)/H_o(f) = A_1(f)$ in decibels is shown in Figure 4.

(e) Fields on the Outside Surfaces of the Plates

To obtain the resultant field $E_t(-a;f) = E_o(-a;f) + E_R(-a;f)$ at $x = -a$ and the field $E_T(a;f)$ at $x = a$ in terms of $E_o(f)$, one proceeds as before, to determine and combine the symmetrical and antisymmetrical phase components. The sets of equations (14)-(17) and (29)-(32) still apply. In the symmetrical case the ratios of the electric and magnetic fields at the surface $x = a$ to the amplitude of the incident field are denoted by

$$S_{2E}(f) = \frac{2E^{s}_{y_3}(a;f)}{E_o(f)} = \frac{C_4 e^{j\beta a} + C_5 e^{-j\beta a}}{C_4} \tag{39a}$$

$$S_{2H}(f) = \frac{2H^{s}_{z_3}(a;f)}{H_o(f)} = -\left[\frac{C_4 e^{j\beta a} - C_5 e^{-j\beta a}}{C_4}\right] = -\left[2e^{j\beta a} - S_{2E}(f)\right]. \tag{39b}$$

*The quantities given are $20 \log_{10}\left[E_i(x;f)/E_o(f)\right]$.

In the antisymmetrical case the corresponding ratios are

$$A_{2E}(f) = -\left[\frac{2E^a_{y_3}(a;f)}{E_o(f)}\right] = \frac{C'_4 e^{j\beta a} + C'_5 e^{-j\beta a}}{C'_4} \tag{40a}$$

$$A_{2H}(f) = \frac{2H^a_{z_3}(a;f)}{H_o(f)} = \frac{C'_4 e^{j\beta a} - C'_5 e^{-j\beta a}}{C'_4} = 2e^{j\beta a} - A_{2E}(f). \tag{40b}$$

By superposition, the electric fields at the outside surfaces $x = \pm a$ due to a single incident field $E_o(f)e^{-j\beta x}$ are:

$$\left.\begin{matrix} E_T(a;f) \\ E_t(-a;f) \end{matrix}\right\} = E^s_{y_3}(a;f) \pm E^a_{y_3}(a;f) = \frac{E_o(f)}{2}\left[S_{2E}(f) \mp A_{2E}(f)\right]. \tag{41}$$

The associated magnetic fields are:

$$\left.\begin{matrix} H_T(a;f) \\ H_t(-a;f) \end{matrix}\right\} = \frac{H_o(f)}{2}\left[A_{2H}(f) \pm S_{2H}(f)\right] = \begin{cases} \dfrac{H_o(f)}{2}\left[S_{2E}(f) - A_{2E}(f)\right] \\ \dfrac{H_o(f)}{2}\left[4e^{j\beta a} - A_{2E}(f) - S_{2E}(f)\right] \end{cases} \tag{42}$$

where, as before, $H_o(f) = E_o(f)/\zeta_o$. It is readily shown that $S_{2E}(f)$ and $A_{2E}(f)$ are

$$S_{2E}(f) = 2\zeta\left[\frac{(\zeta_o \cos\beta b \cos kd - \zeta \sin\beta b \sin kd)(\cos\beta a + j\sin\beta a)}{\zeta\zeta_o(\cos\beta b + j\sin\beta b)\cos kd + j\left(\zeta_o^2 \cos\beta b + j\zeta^2 \sin\beta b\right)\sin kd}\right] \tag{43}$$

and

$$A_{2E}(f) = j2\zeta\left[\frac{(\zeta_o \sin\beta b \cos kd + \zeta \cos\beta b \sin kd)(\cos\beta a + j\sin\beta a)}{\zeta\zeta_o(\cos\beta b + j\sin\beta b)\cos kd + j\left(\zeta^2 \cos\beta b + j\zeta_o^2 \sin\beta b\right)\sin kd}\right]. \tag{44}$$

Explicit expressions for $S_{2H}(f)$ and $A_{2H}(f)$ can be obtained from (39b) and(40b) with (43) and (44).

Graphs of the ratios $E_t(-a;f)/E_o(f)$ and $E_T(a;f)/E_o(f)$ in decibels are shown, respectively, in Figures 5 and 6.

(f) Limiting Forms of the S(f) and A(f) Functions when f = 0

As the frequency approaches zero, $\cos\beta b \to 1$, $\sin\beta b \to \beta b$, $\cos kd \to 1$, $\sin kd \to kd$, also $k/\zeta = -j\sigma$. From (22), (34), (43), and (44) it follows that

$$S_1(0) \to \frac{1}{1 + \zeta_o \sigma d} \tag{45a}$$

$$A_1(0) \to 1 \tag{45b}$$

$$S_{2E}(0) \to \frac{2}{1 + \zeta_o \sigma d} \tag{45c}$$

$$A_{2E}(0) \to 0 \tag{45d}$$

$$S_{2H}(0) = S_{2E}(0) - 2 \to - \frac{2\zeta_o \sigma d}{1 + \zeta_o \sigma d} \tag{45e}$$

$$A_{2H}(0) = 2 - A_{2E}(0) \to 2. \tag{45f}$$

Shielding of the incident field is due to two effects. One of these is skin effect, the other is the reflection that takes place at the outside surface of the shield. The more important attenuating mechanism at low frequencies is reflection. With (45a-f) it follows from (37), (38), (41), and (42) that

$$\frac{E_i(x;0)}{E_o(0)} = S_1(0) = \frac{1}{1 + \zeta_o \sigma d} \tag{46a}$$

$$\frac{H_i(x;0)}{H_o(0)} = A_1(0) = 1 \tag{46b}$$

$$\frac{E_t(-a;0)}{E_o(0)} = \frac{1}{2}\left[S_{2E}(0) + A_{2E}(0)\right] = \frac{1}{1 + \zeta_o \sigma d} \tag{46c}$$

$$\frac{H_t(-a;0)}{H_o(0)} = \frac{1}{2}\left[A_{2H}(0) - S_{2H}(0)\right] = \frac{1 + 2\zeta_o \sigma d}{1 + \zeta_o \sigma d} \tag{46d}$$

$$\frac{E_T(a;0)}{E_o(0)} = \frac{1}{2}\left[S_{2E}(0) - A_{2E}(0)\right] = \frac{1}{1 + \zeta_o \sigma d} \tag{46e}$$

$$\frac{H_T(a;0)}{H_o(0)} = \frac{1}{2}\left[A_{2H}(0) + S_{2H}(0)\right] = \frac{1}{1 + \zeta_o \sigma d} \tag{46f}$$

Note that when $\sigma \to \infty$ for perfectly conducting walls, all ratios vanish except $H_t(-a;0)/H_o(0) = 2$ and $H_i(x;0)/H_o(0) = 1$. Note that in this latter case the amplitude of the incident field on each side of the cavity is $\frac{1}{2}H_o(0)$.

(g) Simplification and Application of the General Formulas

The numerical computations represented in the graphs in Figures 3 to 6 have been made to determine the shielding properties of a region of thickness $2b = 36$ inches $\doteq 0.9144$ m bounded by two infinite aluminum plates of conductivity 3.72×10^7 mho/m with the three thicknesses $d = 1/8$ inch, $1/16$ inch, and $1/32$ inch or $d = 3.175 \times 10^{-3}$, 1.588×10^{-3}, and 0.7938×10^{-3} m. The relevant steady-state frequency range is $f \leq 10^5$ c/sec and for the Gaussian pulses that characterize the transient fields

the upper frequency limit is in this range. The skin depth $\delta = (2/\omega\mu\sigma)^{1/2}$ of aluminum is approximately 2.609×10^{-2} m at f = 10 c/sec, 2.609×10^{-3} m at $f = 10^3$ c/sec, and 2.609×10^{-4} m at $f = 10^5$ c/sec. It is to be noted that at f = 10 c/sec the thickness of the thinnest plate is only about 3 hundredths of the skin depth, whereas at $f \geq 10^4$ c/sec even the thinnest plate is much thicker than the skin depth.

The complex propagation constant $k = (1 - j)/\delta = 12.12(1 - j)\sqrt{f}$ for aluminum (with $\sigma = 3.72 \times 10^7$ mho/m) ranges from $k = 38.33(1 - j)$ at f = 10 c/sec to $k = 3.833(1 - j) \times 10^3$ at $f = 10^5$ c/sec. Over the range $10 \leq f \leq 10^5$,

$$|k| >> \beta \tag{47}$$

where $\beta = \omega\sqrt{\mu_o \epsilon_o} = 2.094 \times 10^{-8} f$. Note also that the electrical distance $\beta b = 0.9574 \times 10^{-8} f$ satisfies the inequality

$$\beta b << 1 \tag{48}$$

over the entire frequency range. On the other hand, kb extends from $(1 - j)17.52$ at f = 10 c/sec to $(1 - j)1.752 \times 10^3$ at $f = 10^5$ c/sec.

Since

$$k\zeta = \beta\zeta_o = \omega\mu_o \tag{49}$$

it follows from (47) that

$$\zeta_o >> |\zeta|. \tag{50}$$

Over the range of frequencies defined by

$$|\tan kd| >> \frac{|\zeta|}{\zeta_o} = \frac{\beta}{|k|} \tag{51}$$

the general formulas for $S_1(f)$, $A_1(f)$, $S_2(f)$, and $A_2(f)$ may be simplified greatly. Note that for the thinnest plate when f = 10 c/sec, $kd = (1 - j)3.043 \times 10^{-2}$ and $\beta/k = \frac{5.463}{(1 - j)} \times 10^{-9}$; when $f = 10^5$ c/sec, $kd = 3.043(1 - j)$ and $\beta/k = \frac{5.463}{(1 - j)} \times 10^{-7}$, so that (51) is satisfied in the entire range $10 \leq f \leq 10^5$. The appropriate specific formulas for the several ratios are

$$S_1(f) \doteq \frac{-j\beta}{k \sin kd} \tag{52}$$

$$A_1(f) \doteq \frac{1}{\cos kd - kb \sin kd} \tag{53}$$

$$S_{2E}(f) \doteq \frac{-j2\beta}{k \tan kd} \tag{54}$$

$$A_{2E}(f) \doteq \frac{j2\beta}{k}\left[\frac{kb \cos kd + \sin kd}{\cos kd - kb \sin kd}\right]. \tag{55}$$

As before $S_{2H}(f) = S_{2E}(f) - 2$, $A_{2H}(f) = 2 - A_{2E}(f)$. With these values, (37) and (38) give the field in the cavity to be

$$E_i(x;f) = \frac{-jE_o(f)\beta}{k}\left[\frac{1}{\sin kd} + \frac{kx}{\cos kd - kb \sin kd}\right] \tag{56a}$$

$$H_i(x;f) = H_o(f)\left[\frac{1}{\cos kd - kb \sin kd} - \frac{\beta^2 x}{k \sin kd}\right]$$

$$\doteq \frac{H_o(f)}{\cos kd - kb \sin kd}. \tag{56b}$$

It follows that

$$E_i(0;f) = \frac{-jE_o(f)\beta}{k \sin kd} \tag{57}$$

and

$$E_i(b;f) = \frac{-j\beta}{k} E_o(f)\left[\frac{\cos kd}{\sin kd(\cos kd - kb \sin kd)}\right] \tag{58a}$$

$$E_i(-b;f) = \frac{-j\beta}{k} E_o(f)\left[\frac{\cos kd - 2kb \sin kd}{\sin kd(\cos kd - kb \sin kd)}\right]. \tag{58b}$$

Similarly,

$$H_i(0;f) \doteq H_i(b;f) \doteq H_i(-b;f) \doteq \frac{H_o(f)}{\cos kd - kb \sin kd}. \tag{59}$$

From (41), the total field at $x = \pm a$ is

$$\left.\begin{matrix} E_T(a;f) \\ E_t(-a;f) \end{matrix}\right\} = \frac{-j\beta}{k} E_o(f)\left[\cot kd \pm \frac{kb \cos kd + \sin kd}{\cos kd - kb \sin kd}\right] \tag{60a}$$

so that with (42) the field on the far outside is

$$\frac{E_T(a;f)}{E_o(f)} = \frac{H_T(a;f)}{H_o(f)} = \frac{-j\beta}{k}\left[\frac{1}{\sin kd(\cos kd - kb \sin kd)}\right]. \tag{60b}$$

On the near outside it is

$$\frac{E_t(-a;f)}{E_o(f)} = \frac{-j\beta}{k}\left[\frac{\cos 2kd - kb \sin 2kd}{\sin kd(\cos kd - kb \sin kd)}\right] \tag{60c}$$

and

$$\frac{H_t(-a;f)}{H_o(f)} = 2 - \frac{E_t(-a;f)}{E_o(f)} . \tag{60d}$$

A clear picture of the action of the two plates as shields is obtained with the thicker shields at the higher frequencies included in the range for which (52)-(55) are valid. Specifically, when the additional restriction $|k|d \geq 1.5$ is satisfied, the approximation

$$\sin kd \doteq \frac{1}{2} e^{jkd} \doteq \cos kd \tag{61}$$

is a good one.

With (61) and $|k|b >> 1$ the following illuminating formulas for the fields between the plates and on their outside surfaces are obtained:

$$\frac{E_i(x;f)}{E_o(f)} \doteq \frac{-j2\beta}{k}\left(1 - \frac{kx}{kb - 1}\right)e^{-jkd} \tag{62}$$

$$\frac{H_i(x;f)}{H_o(f)} \doteq -\frac{2e^{-jkd}}{kb - 1} \tag{63}$$

$$\frac{E_t(-a;f)}{E_o(f)} \doteq \frac{-j2\beta}{k}; \quad \frac{H_t(-a;f)}{H_o(f)} = 2\left(1 + j\frac{\beta}{k}\right) \tag{64}$$

$$\frac{E_T(a;f)}{E_o(f)} = \frac{H_T(a;f)}{H_o(f)} = \frac{j4\beta}{k}\frac{e^{-j2kd}}{kb - 1} . \tag{65}$$

In the range for which these formulas are valid the approximation $|kb| >> 1$ is also valid. These formulas are useful in an interpretation of the upper frequency ranges in Figures 3 to 6. Note that from (62)

$$\frac{E_i(-b;f)}{E_o(f)} = \frac{-j2\beta}{k}\left[\frac{2kb - 1}{kb - 1}\right]e^{-jkd} \doteq \frac{-j4\beta}{k} e^{-jkd} \tag{66a}$$

$$\frac{E_i(0;f)}{E_o(f)} = S_1(f) = \frac{-j2\beta}{k} e^{-jkd} \tag{66b}$$

$$\frac{E_i(b;f)}{E_o(f)} = \frac{j2\beta}{k}\frac{e^{-jkd}}{kb - 1} \doteq \frac{j2\beta}{k^2 b} e^{-jkd} \tag{66c}$$

where the formulas on the right assume that $|kb| >> 1$. These formulas all give the same exponential decay due to the thickness of a single sheet characteristic of the upper frequency ranges of Figures 3a, b, c.

The small difference in magnitude (only a factor of 2) between $E_i(-b;f)/E_o(f)$ and $E_i(0;f)/E_o(f)$ is clear in Figures 3a and 3b. The much greater decrease in amplitude due to the large extra factor kb in the denominator of $E_i(b;f)/E_o(f)$ is evident in Figure 3c. Note that $E_i(0;f)$ is due entirely to the symmetrically excited part of the field which is essentially constant across the interior of the shield. The antisymmetrical part vanishes at the center, effectively adds to the symmetrically excited part for $-a \leq x < 0$ and subtracts from this for $0 < x \leq a$. The part of the magnetic field due to the symmetrical electric field excitation is negligible in the upper frequency range whereas the field due to antisymmetrical electric field excitation is essentially constant across the interior of the shield. It is exponentially attenuated by one plate but has no factors of small magnitude (β/k or $1/kb$) as does the electric field. In the lower frequency range where (56)-(60) must be used instead of (62)-(65), the attenuation through the plates is not exponential and may be quite small. It is given by (56b) and shown in Figure 4.

The ratio $E_t(-a;f)/E_o(f)$ at the front outer surface of the plates and represented in Figure 5 involves no exponential attenuation, but is very small owing to the high conductivity of the aluminum which produces a large reflection in nearly opposite phase. The magnetic field, on the other hand, is reflected nearly in phase and its amplitude is almost doubled as may be seen from (64).

The ratio $E_T(a;f)/E_o(f)$ or $H_T(a;f)/H_o(f)$ given in (65) is attenuated exponentially by e^{-j2kd}; i.e., by the two plates, and in addition has the large factor kb in the denominator. This agrees with Figure 6. If the conductivity of the plates is made infinite so that $\sigma \to \infty$, it follows that $E_i(x;f) = H_i(x;f) = E_T(a;f) = H_T(a;f) = E_t(-a;f) = 0$, $H_t(-a;f) = 2$.

4. The Form of the Integrals to be Evaluated by a Computer

The description of the incident electric field pulse assumed in this paper is

$$e_o(t) = Ae^{-t^2/2t_1^2} \tag{67}$$

where A is the value of $e_o(0)$ in volts/m, t is the time, and t_1 is a measure of the pulse width. The spectrum of this pulse is

$$E_o(f) = At_1\sqrt{2\pi}e^{-f^2/2f_1^2}. \tag{68}$$

In this expression f is the frequency in cycles/sec, and $f_1 = 1/2\pi t_1$.

Let $G(x;f) = G_R(x;f) + jG_I(x;f)$ represent a desired steady-state shielding ratio, such as $E_i(x;f)/E_o(f)$. The time history of the electric field in the cavity at point x is then

$$e_i(x;t) = \int_{-\infty}^{\infty} G(x;f)E_o(f)e^{j2\pi ft}\,df$$

$$\approx 2At_1\sqrt{2\pi}\int_0^{f_c}\left[G_R(x;f)\cos 2\pi ft - G_I(x;f)\sin 2\pi ft\right]e^{-f^2/2f_1^2}\,df \tag{69}$$

where, to a good approximation, $f_c = 2.6\, f_1$. In the last expression use has been made of the relation $G^*(f) = G(-f)$. This is the form of the integral that has been evaluated on the computer. For computations of the electric field the constant A in (69) was taken to be 1 volt per meter; for computations of the magnetic field, h and H are substituted in (67) to (69) in place of e and E and A is set equal to 1 ampere per meter.

The time histories of the electric and magnetic fields in and outside the cavity are exhibited in a series of graphs for a particular cavity (of length 36 inches with the three wall thicknesses 1/32 inch, 1/16 inch, and 1/8 inch) when an electromagnetic field with an amplitude distribution in the form of a Gaussian pulse is incident from one side. A number of pulse lengths from $t_1 = 6\ \mu$sec to 48 μsec are used.

In order to understand the variation in time of the electric and magnetic fields in the cavity it is important to note that even for the shortest pulses used in the calculations, ($t_1 = 6\ \mu$sec) the pulse width t_1 is very great compared to the time of transit of the pulse across the cavity, viz., $t = 0.9144/(3 \times 10^8)$ sec $= 0.00348\ \mu$sec. *It follows that the field is reflected back and forth in the cavity many times even during the time* t_1. *The instantaneous field is then a superposition of these multiply reflected components. It is also significant to note that for the lower frequencies and the thinnest plates the attenuation through the plates is relatively small and shielding is due primarily to reflection.*

In Figures 7a-d, 8a-d, and 9a-d are shown the instantaneous electric fields in the cavity respectively at the points $x = -b$, 0, and b. As is to be expected from the similarity of their steady-state transfer functions, the time histories of the electric fields at $x = -b$ and at $x = 0$ are quite similar. The electric field at the center, $x = 0$, is determined entirely by the steady-state transfer function of the symmetrically excited part of the electric field, that at $x = -b$ is determined from the sum of the steady-state ratio functions of both the symmetrical and antisymmetrical parts of the excitation. On the other hand, at $x = b$, the field is determined from the difference between the steady-state functions of the symmetrical and antisymmetrical excitations. Since this is very small, the instantaneous electric field at $x = -b$ is smaller by a factor near 10^{-3} than the fields at $x = 0$ or $x = b$; it also has a much less significant peak.

Since the steady-state transfer function for the magnetic field in the cavity is predominantly due to the antisymmetrical part of the excitation, and since for this the magnetic field is essentially constant across the cavity, it follows that the time histories of the magnetic fields at all points in the cavity are essentially the same. They are shown in Figures 10a-d on an expanded time scale for short time intervals during which the field increases rapidly and in Figures 11a-d on a more contracted time scale for a much longer time in which the initial increase of the field appears very abrupt but the long slow decay is apparent. It is to be noted that although the ratio $H_i(x;f)/H_o(f)$ is very much greater than $E_i(x;f)/E_o(f)$ since the magnetic field is nearly doubled at each reflection whereas the electric field is almost canceled, the decay rates of electric and magnetic fields must nevertheless be the same. This is considered in greater detail in Section 5.

The electric and magnetic fields beyond the second metal wall, $x \geq a$, constitute an outward traveling disturbance that is not a superposition of incident and reflected components as in front of and inside

the cavity. At every point and instant the ratio of electric to magnetic field is the constant ζ_o, so that the time history of both electric and magnetic fields is the same for $x \geq a$. The instantaneous electric field at $x = a$ is represented in Figures 12a-d. It is seen to be extremely small, nevertheless it necessarily decays as slowly as the field in the cavity. Note that for the broader pulses with larger t_1 the spectrum contains predominantly frequencies that are sufficiently low to make the attenuation through the plates small. Shielding is primarily due to reflection and not significantly due to skin effect. This is shown, for example, by the fact that in Figures 9d and 12d the curves for $e_i(b;t)$ and $e_T(a;t)$ for the fields on the two sides of the second plate differ negligibly for the thinnest plates.

5. Decay Rates in the Cavity

The ratio of decay of the electromagnetic fields in the cavity may be estimated by evaluating the integral (69) for the simplified shielding ratios (52) and (53) and with $E_o(f) = 1$, that is, for a delta-function pulse. For the symmetrical excitation the steady-state shielding ratio is $S_1(f)$ as given in (52); for the antisymmetrical excitation the ratio is $A_1(f)$ as given in (53).

The instantaneous electric field for the symmetric case is

$$\left[e_i(x;t)\right]_{sym} = -j\frac{c}{2\pi}\int_{-\infty}^{\infty}\frac{\beta\cos\beta x}{k\sin kd}e^{j\beta ct}\,d\beta \tag{70a}$$

since $\omega = \beta c$. The simple poles of this integral occur at $\sin kd = 0$ or at

$$k^2d^2 = n^2\pi^2 \text{ or } \beta = \frac{jn^2\pi^2}{d^2\sigma\zeta_o}. \tag{70b}$$

These are all in the upper half of the complex plane so that the contour may be closed in a great semicircle above the real axis. By Cauchy's theorem,

$$\left[e_i(x;t)\right]_{sym} = \left(\frac{-jc}{2\pi}\right)2\pi j(K_1 + K_2 + \cdots + K_n)$$

where the K's are the residues at the poles. The residue K_n may be obtained from the general formula

$$K_n = \left.\frac{\beta e^{j\beta ct}\cos\beta x}{\frac{d}{d\beta}(k\sin kd)}\right|_{\beta = \frac{jn^2\pi^2}{d^2\sigma\zeta_o}}. \tag{71a}$$

Since $k = \sqrt{-j\omega\mu\sigma} = \sqrt{-j\beta\zeta_o\sigma}$, this gives

$$K_n = 2(-1)^{n-1}\frac{n^2\pi^2}{d^3\sigma^2\zeta_o^2}e^{-\frac{n^2\pi^2ct}{d^2\sigma\zeta_o}}\cosh\left(\frac{n^2\pi^2x}{d^2\sigma\zeta_o}\right). \tag{71b}$$

It follows that

$$\left[e_i(x;t)\right]^2_{sym} = \frac{2E_o c\pi^2}{d^3\sigma^2\zeta_o^2} \sum_1^\infty (-1)^{n-1} n^2 \exp\left(\frac{-n^2\pi^2 ct}{d^2\sigma\zeta_o}\right) \cosh\left(\frac{n^2\pi^2 x}{d^2\sigma\zeta_o}\right) \tag{72}$$

The slowest decay is for the term with $n = 1$ for which the decay time is

$$t_s = \frac{\zeta_o \sigma d^2}{\pi^2 c} = 4.736\, d^2 \text{sec} = \begin{cases} 2.984 \times 10^{-6} \text{ sec for } d = 1/32 \text{ inch} \\ 11.94 \times 10^{-6} \text{ sec for } d = 1/16 \text{ inch} \\ 47.74 \times 10^{-6} \text{ sec for } d = 1/8 \text{ inch} \end{cases} \tag{73}$$

The numerical values are for aluminum. This is a measure of the exponential decay of the electric and magnetic fields that are excited in the cavity, in the symmetrical mode of the electric field.

For the antisymmetrical mode,

$$\left[e_i(x;t)\right]_{antisym} = \frac{-jc}{2\pi} \int_{-\infty}^{\infty} \frac{\sin \beta x}{\cos kd - kb \sin kd} e^{j\beta ct}\, d\beta. \tag{74}$$

The poles of this integral occur at the roots of

$$\tan kd = \frac{1}{kb} \text{ or } kd = \frac{\pi}{2} - \tan^{-1} kb. \tag{75a}$$

Since the slowest decay time for the symmetrical excitation has been used as an approximation, the same may be done in this case and only the first root determined. This must occur approximately when

$$k^2 bd = 1 \tag{75b}$$

or, with $k^2 = -j\beta\sigma\zeta_o$, when

$$\beta = \frac{j}{\zeta_o \sigma bd}. \tag{76}$$

The residue at the associated pole is

$$K_1 = \left.\frac{e^{j\beta ct} \sin \beta x}{\frac{d}{d\beta}(\cos kd - kb \sin kd)}\right|_{\beta = \frac{j}{\zeta_o \sigma bd}} \tag{77a}$$

$$\doteq \left.\frac{e^{j\beta ct} \sin \beta x}{\frac{d}{d\beta}(1 - k^2 bd)}\right|_{\beta = \frac{j}{\zeta_o \sigma bd}} \tag{77b}$$

so that

$$K_1 = \frac{\exp\left(\frac{-ct}{\zeta_o \sigma bd}\right)}{\zeta_o \sigma bd} \sinh\left(\frac{x}{\zeta_o \sigma bd}\right). \tag{77c}$$

It follows that

$$\left[e_i(x;t)\right]_{\text{antisym}} = \frac{c}{\zeta_o \sigma bd} \exp\left(\frac{-ct}{\zeta_o \sigma bd}\right) \sinh\left(\frac{x}{\zeta_o \sigma bd}\right) \tag{78}$$

+ contributions from higher-order poles.

The slowest decay time of the antisymmetrical mode is

$$t_A = \frac{\zeta_o \sigma bd}{c} = 46.75\ bd \text{ sec} = \begin{cases} 1.697 \times 10^{-2} \text{ sec for } d = 1/32 \text{ inch} \\ 3.394 \times 10^{-2} \text{ sec for } d = 1/16 \text{ inch} \\ 6.786 \times 10^{-2} \text{ sec for } d = 1/8 \text{ inch} \end{cases} \tag{79}$$

The ratio of the two decay times is

$$\frac{t_A}{t_S} = \frac{\zeta_o \sigma bd}{c} \frac{\pi^2 c}{\zeta_o \sigma d^2} = \frac{\pi^2 b}{d}. \tag{80}$$

For the three thicknesses d = 1/32 inch, 1/16 inch, and 1/8 inch and the distance b = 18 inches between plates, the ratios are:

d	b/d	$\pi^2 b/d$
1/32 inch	32 x 18	5685
1/16 inch	16 x 18	2842
1/8 inch	8 x 18	1421

(81)

It is clear that the antisymmetrical mode is damped out very much more slowly than the symmetrical mode, so that when the two are superimposed to give the response for a disturbance incident from the one side only, the contribution from the symmetrical part of the excitation dies out very quickly and only the response from the antisymmetrical part of the excitation persists. It is important to note that as a consequence of symmetry the antisymmetric odd electric field and the symmetric odd magnetic field are identically zero at the center of the cavity where x = 0. It follows that at this point, the total magnetic field decays slowly, the total electric field rapidly. This difference in rates of decay is seen in Figures 8a and 11a. At all other points the decay rates of the total electric and magnetic fields involve the independent decay of the electric and magnetic components of both symmetries. Ultimately, the rate of decay is that of the antisymmetric components with odd electric and even magnetic fields. This may be seen from a comparison of Figures 10a and 11a which show the slow decay of the antisymmetrical parts of the electric and associated magnetic fields after the rapid decay of the symmetrical parts. The decay rate is easily estimated from Figure 11a where for the thinnest plate the amplitude clearly decreases to about 1/e or 1/2.7 of its maximum value in about 16 milliseconds in agreement with (79).

6. Conclusion

A complete picture has been obtained of the shielding provided by a parallel-plate region to incident pulses of Gaussian shape both in theoretical and numerical form. These results are useful in estimating the efficacy as shields of metal containers of finite size only insofar as no resonances are excited that involve standing waves of current along the metal walls. At resonant frequencies the large currents induced in the walls of the shield are associated with correspondingly large resonant fields.[1]

Supplemental References

1. Anderson, W. L., and Moore, R. K., "Frequency Spectra of Transient Electromagnetic Pulses in a Conducting Medium," IRE Transactions on Antennas and Propagation, **AP-8**, pp. 603-607, November 1960.

2. Harrison, C. W., Jr., "Transient Electromagnetic Field Propagation Through Infinite Sheets, into Spherical Shells, and into Hollow Cylinders," Submitted for publication in IEEE Transactions on Antennas and Propagation.

3. Harrison, C. W., Jr., and King, R. W. P., "Response of a Loaded Electric Dipole in an Imperfectly Conducting Cylinder of Finite Length," Journal of Research of the National Bureau of Standards-D. Radio Propagation, **64D**, No. 3, pp. 289-293, May-June 1960.

4. King. L. V., "Electromagnetic Shielding at Radio Frequences," Philosophical Magazine and Journal of Science, **15**, No. 97, pp. 201-223, February 1933.

5. Richards, P. I., "Transients in Conducting Media," IRE Transactions on Antennas and Propagation, **AP-6**, pp. 178-182, April 1958.

6. Wait, J. R., "Shielding of a Transient Electromagnetic Dipole Field by a Conductive Sheet," Canadian Journal of Physics, **34**, pp. 890-893, 1956.

7. Wait, J. R., "Induction in a Conducting Sheet by a Small Current Carrying Loop," Applied Science Research B3, p. 230, 1953.

8. Zisk, S. H., "Electromagnetic Transients in Conducting Media," IRE Transactions on Antennas and Propagation, **AP-8**, pp. 229-230, March 1960.

9. Zitron, N. R., "Shielding of Transient Electromagnetic Signals by a Thin Conducting Sheet," Journal of Research of the NBS-D. Radio Propagation, **64D**, No. 5, pp. 563-567, September-October 1960.

[1] King, R. W. P., and Harrison, C. W., Jr., "Cylindrical Shields," IRE Transactions on Antennas and Propagation, **AP-9**, No. 2, pp. 166-170, March 1961.

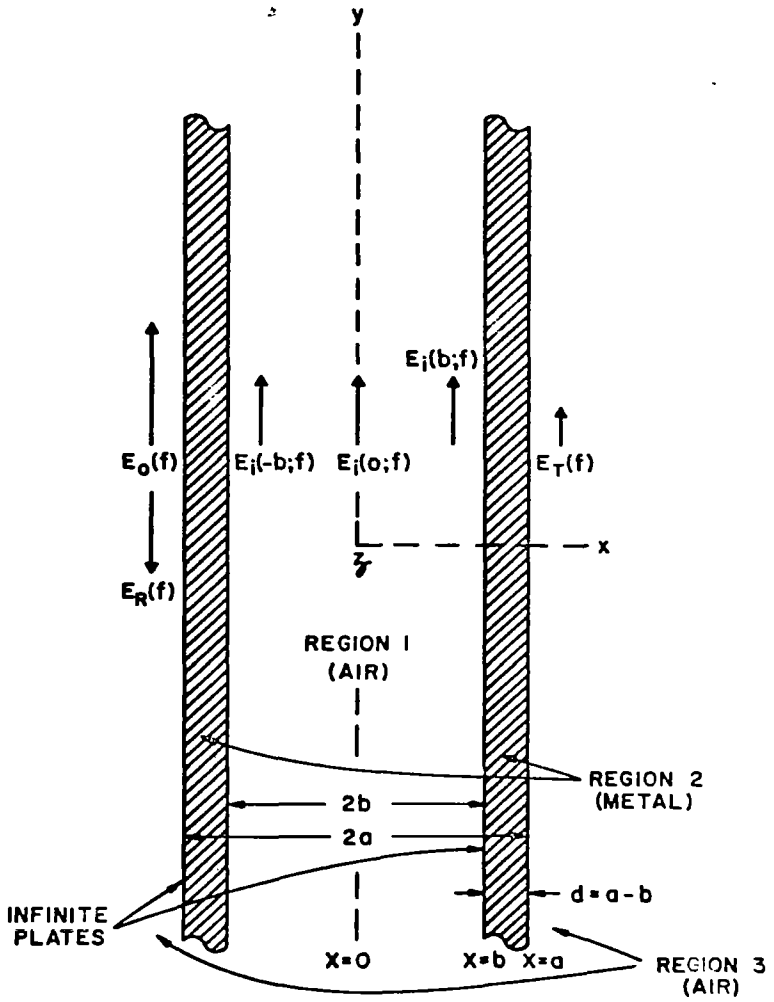

Figure 1. Dual Plate Shield

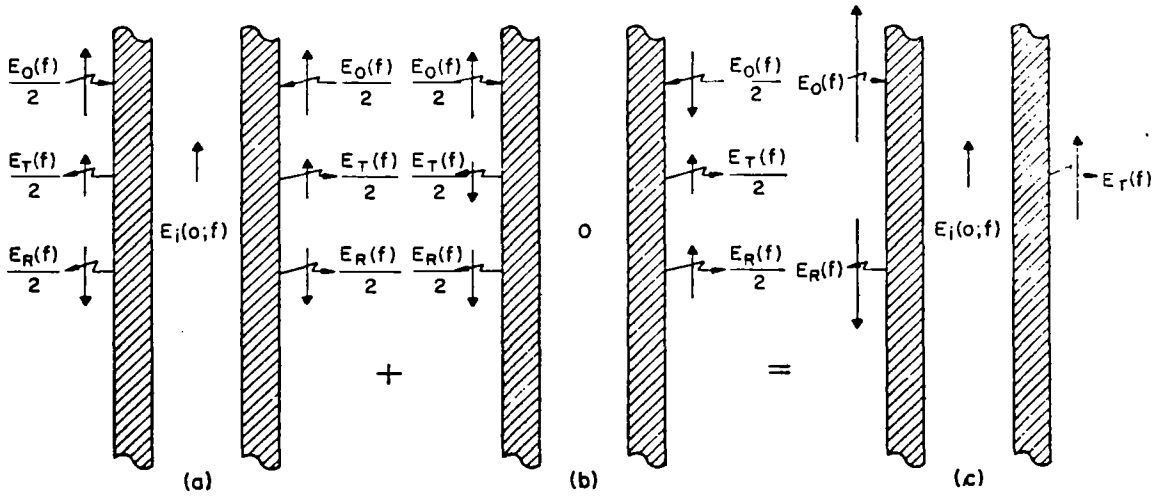

Figure 2. Use of Symmetrical Phase Components to Solve the Dual Plate Shield Problem Illustrated by Figure 1

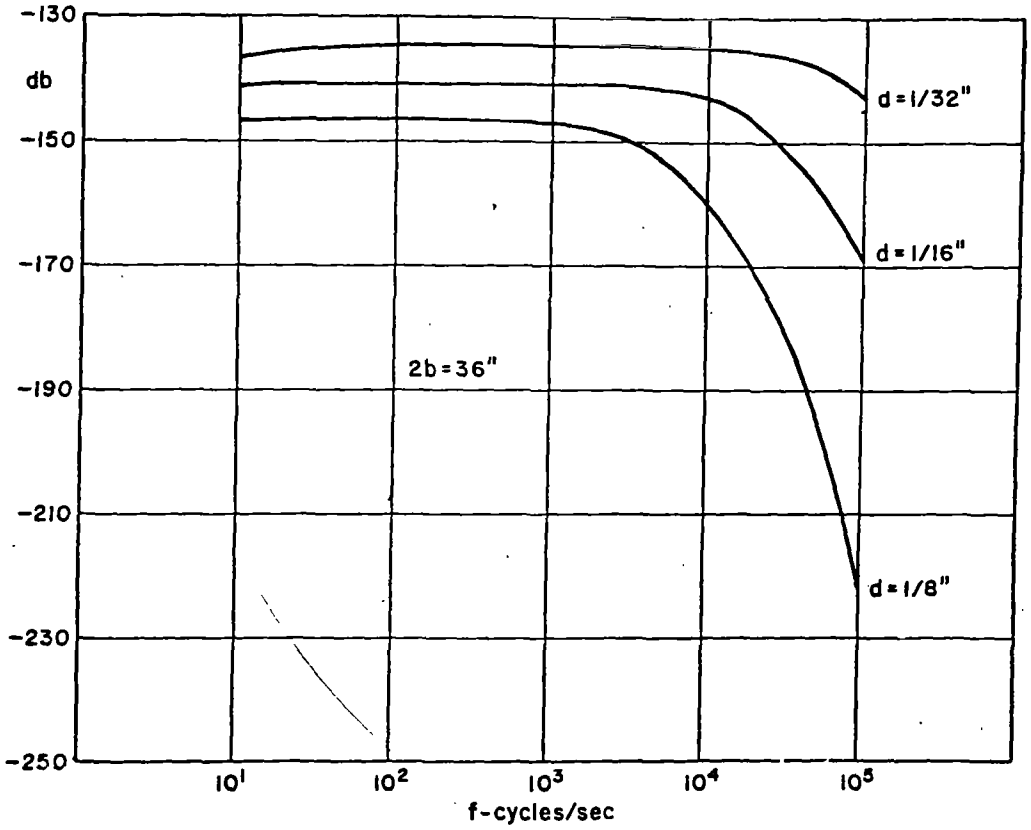

Figure 3a. Dual Plate Shield. Steady State Function Relating $E_i(-b;f)$ to $E_o(f)$

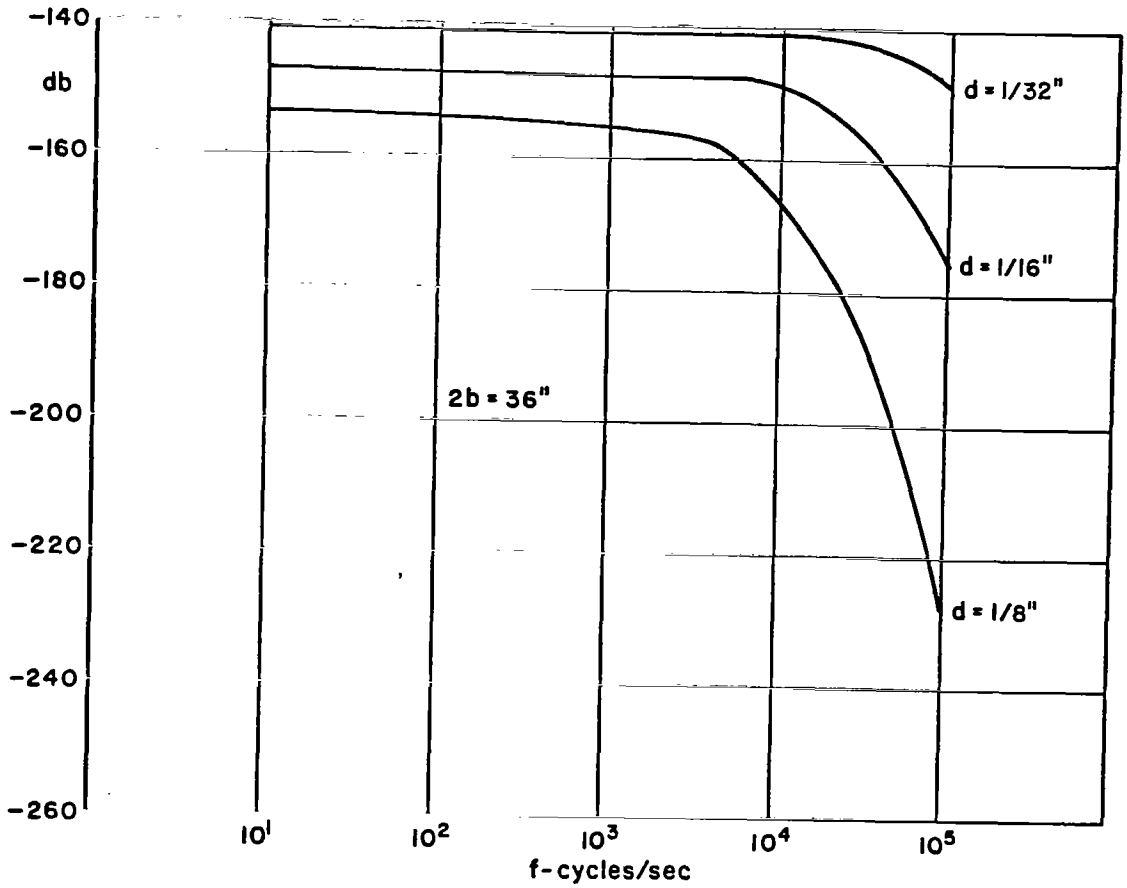

Figure 3b. Dual Plate Shield. Steady State Transfer Function Relating $E_i(0;f)$ to $E_o(f)$

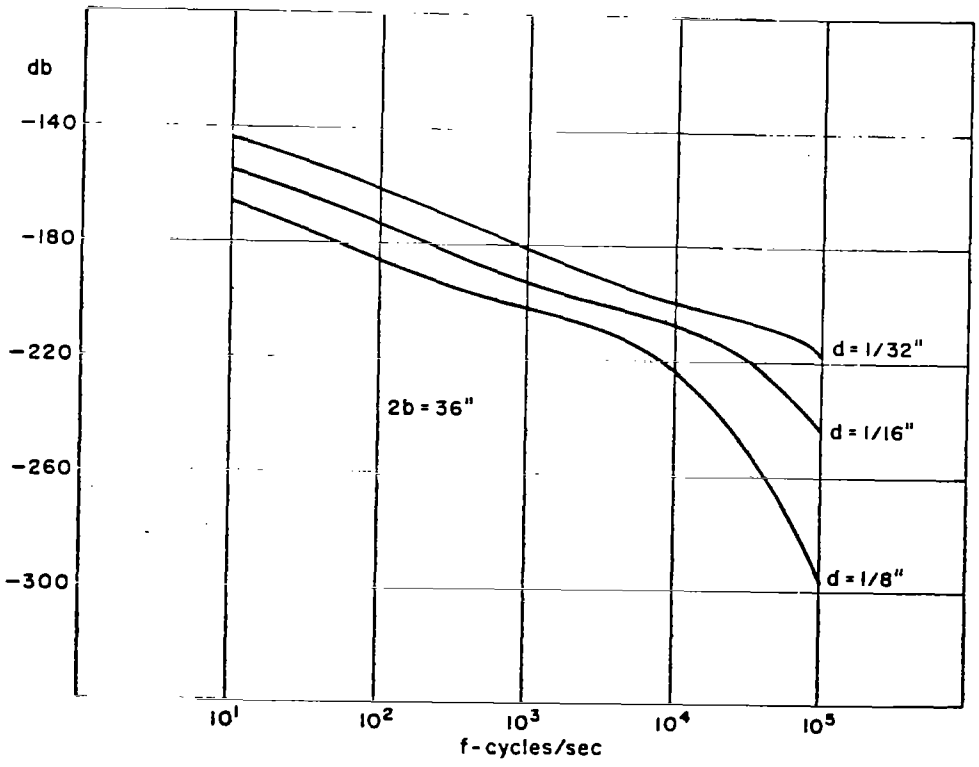

Figure 3c. Dual Plate Shield. Steady State Transfer Function Relating $E_i(b;f)$ to $E_o(f)$

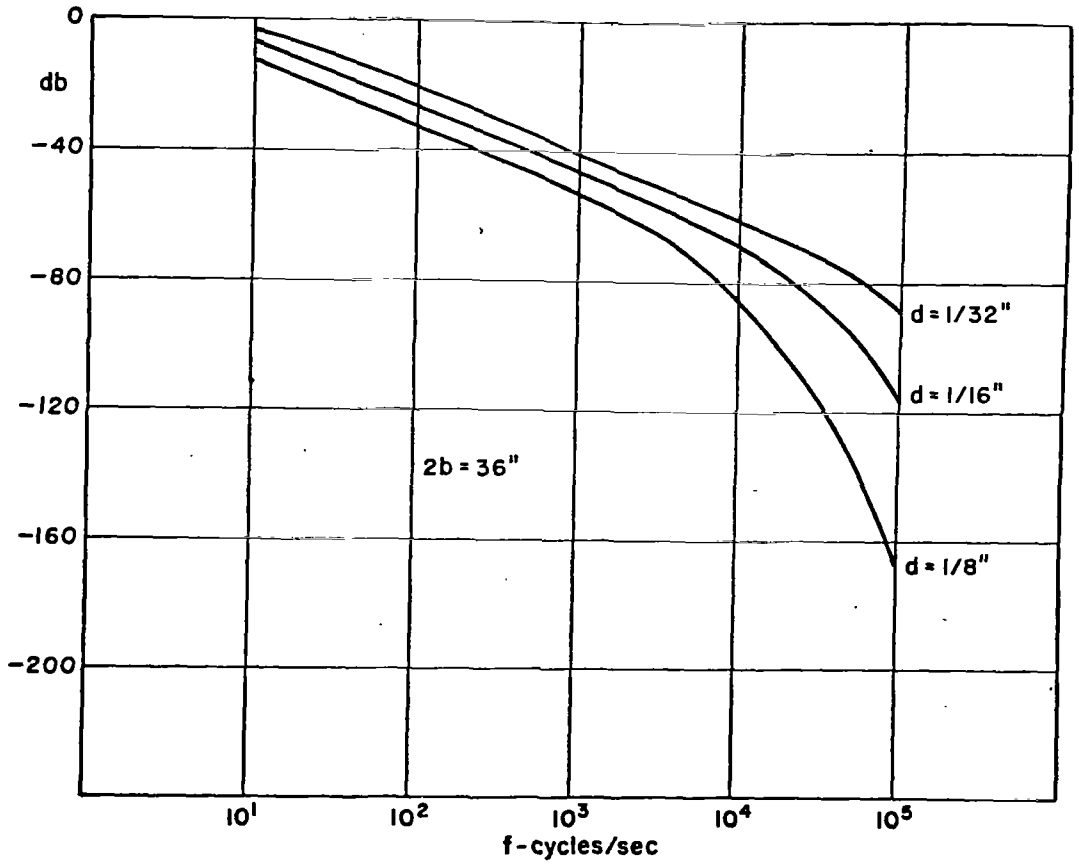

Figure 4. Dual Plate Shield. Steady State Transfer Function Relating $H_i(0;f)$ to $H_o(f)$

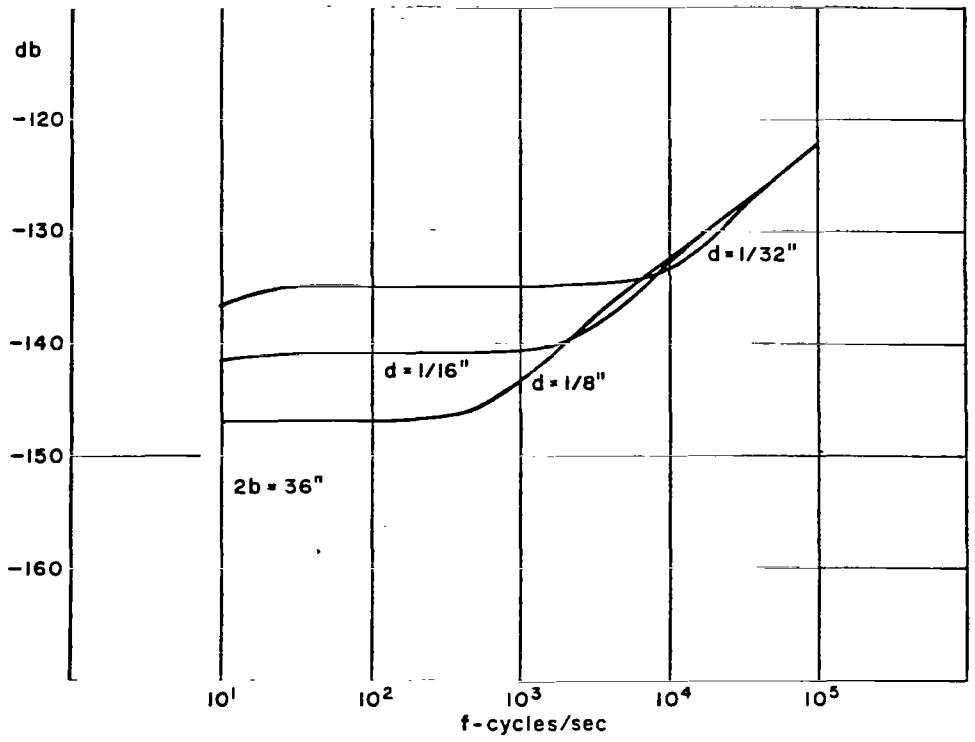

Figure 5. Dual Plate Shield. Steady State Transfer Function Relating $E_t(-a;f)$ to $E_o(f)$

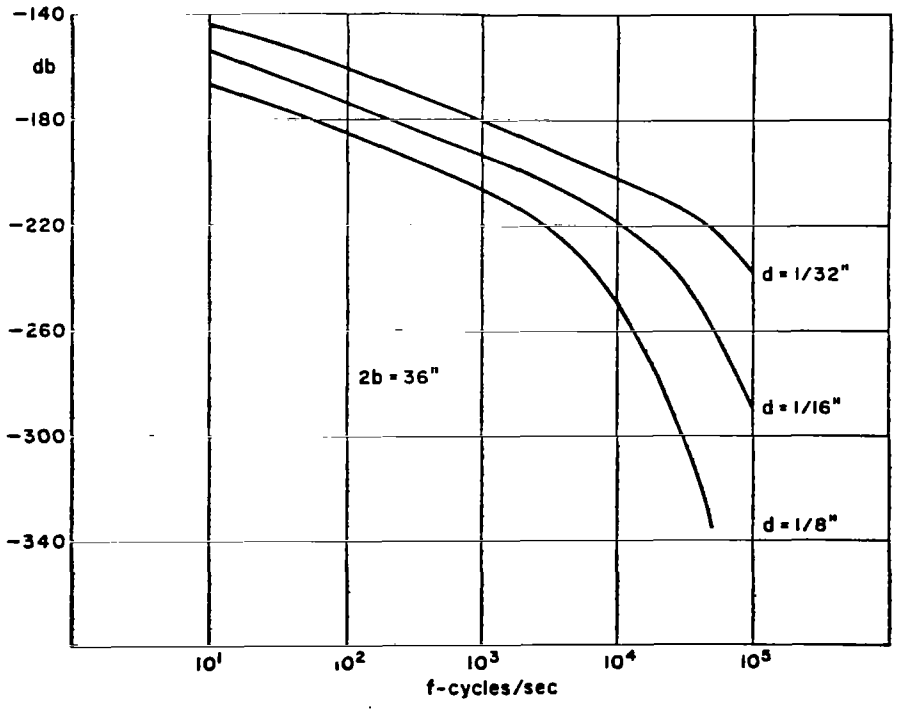

Figure 6. Dual Plate Shield. Steady State Transfer Function Relating $E_T(a;f)$ to $E_o(f)$

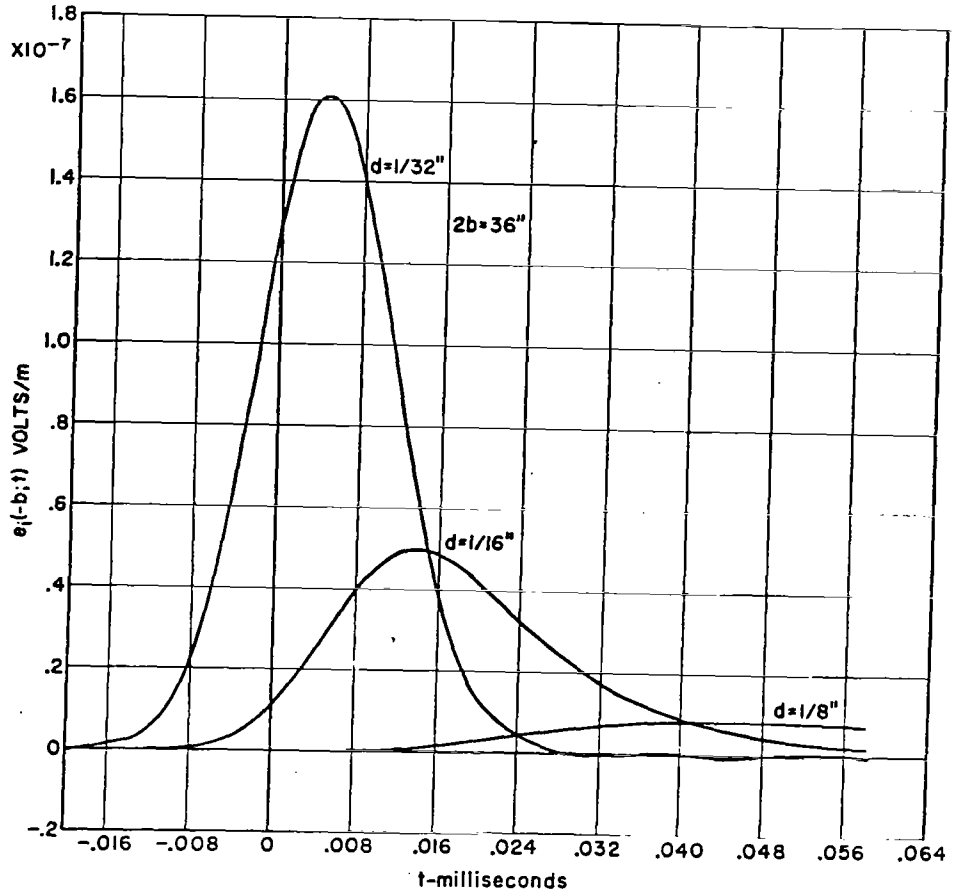

Figure 7a. Dual Plate Shield. $e_o(0) = 1$ volt/m, $t_1 = 6\ \mu s$

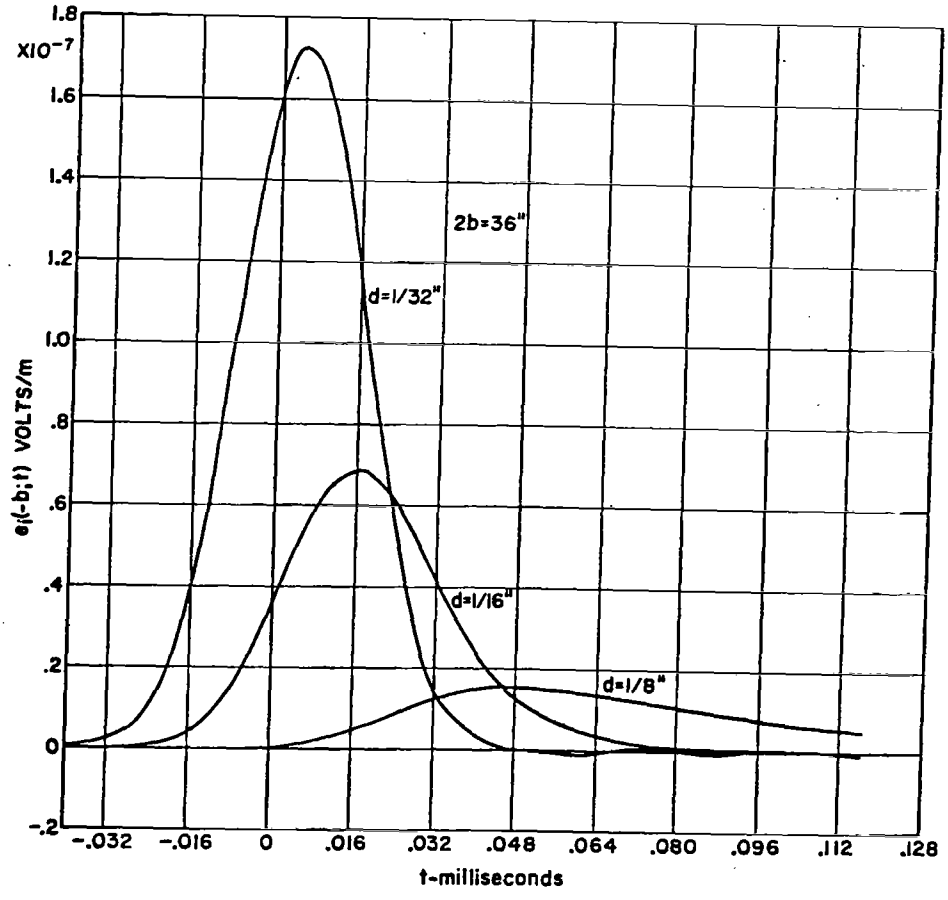

Figure 7b. Dual Plate Shield. $e_o(0) = 1$ volt/m, $t_1 = 12\ \mu s$

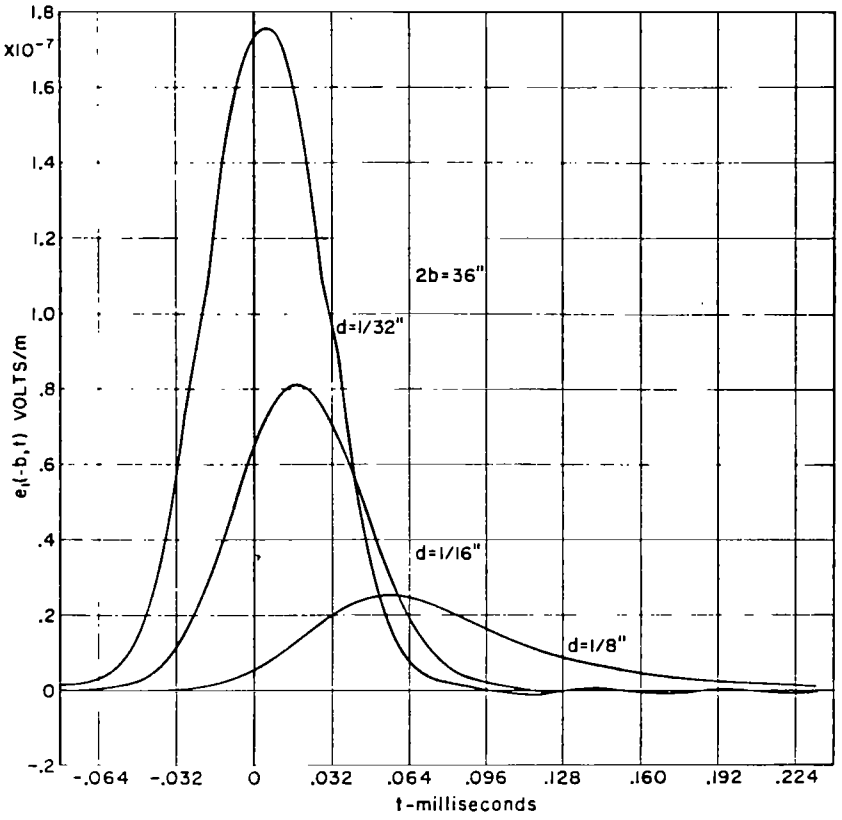

Figure 7c. Dual Plate Shield. $e_o(0)$ = 1 volt/m, t_1 = 24 μs

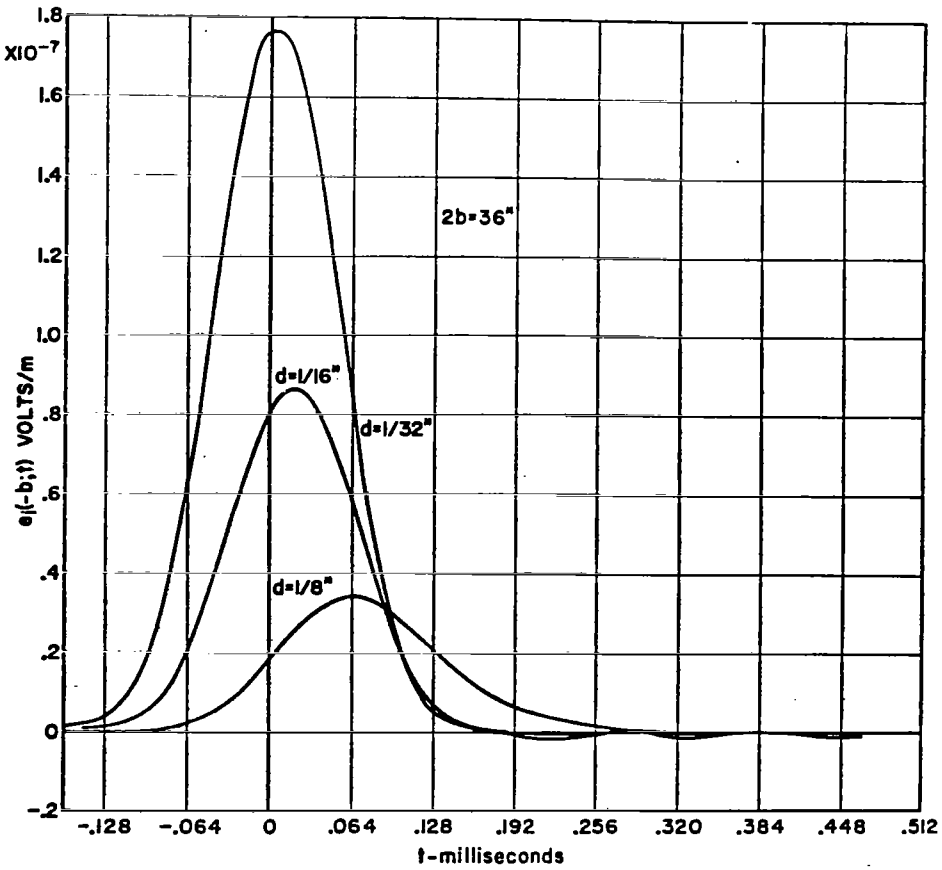

Figure 7d. Dual Plate Shield. $e_o(0)$ = 1 volt/m, t_1 = 48 μs

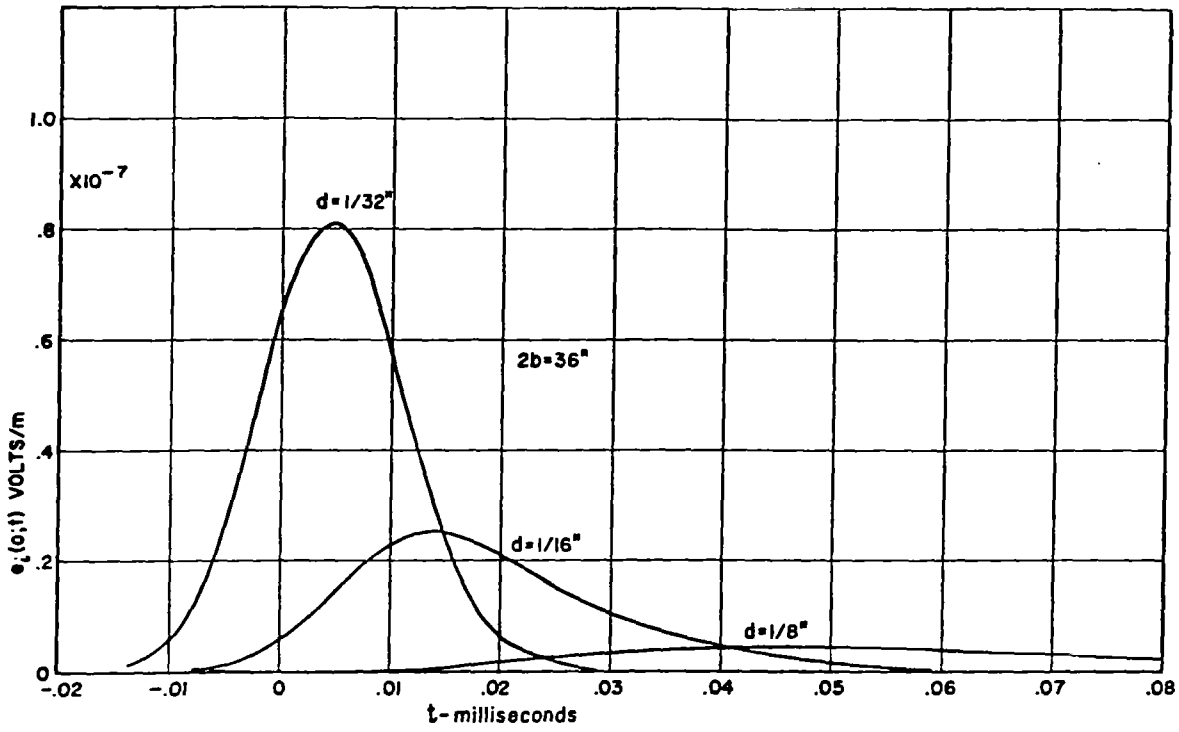

Figure 8a. Dual Plate Shield. $e_o(0) = 1$ volt/m, $t_1 = 6\ \mu s$

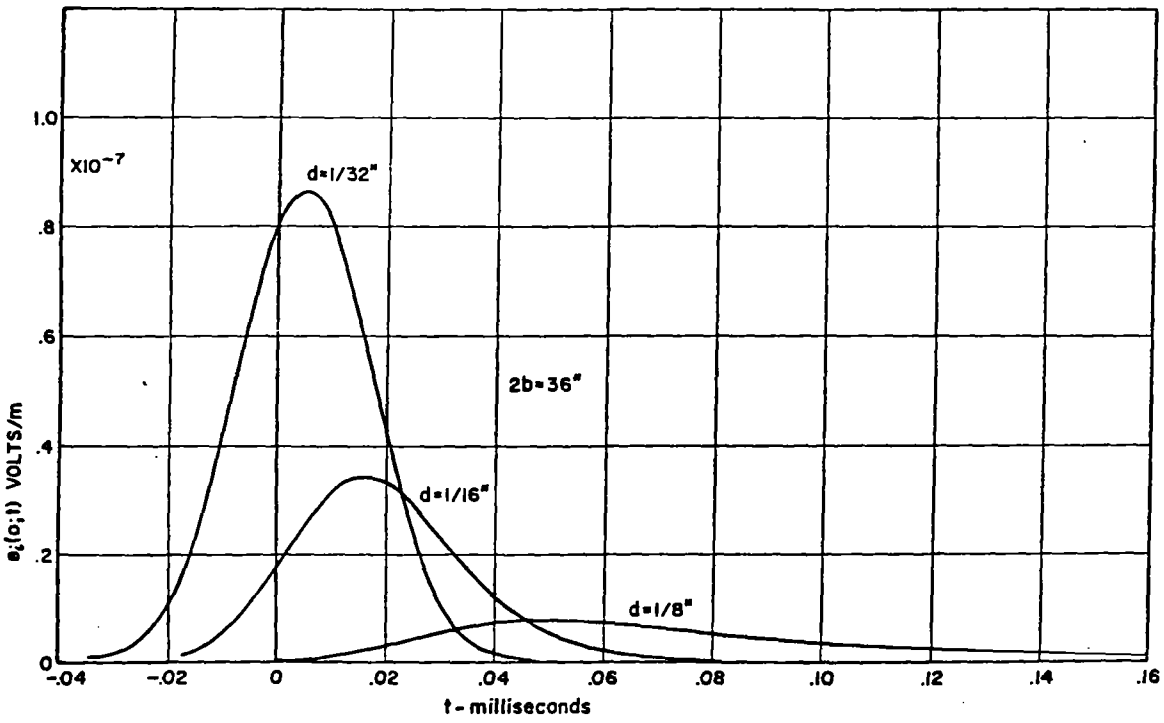

Figure 8b. Dual Plate Shield. $e_o(0) = 1$ volt/m, $t_1 = 12\ \mu s$

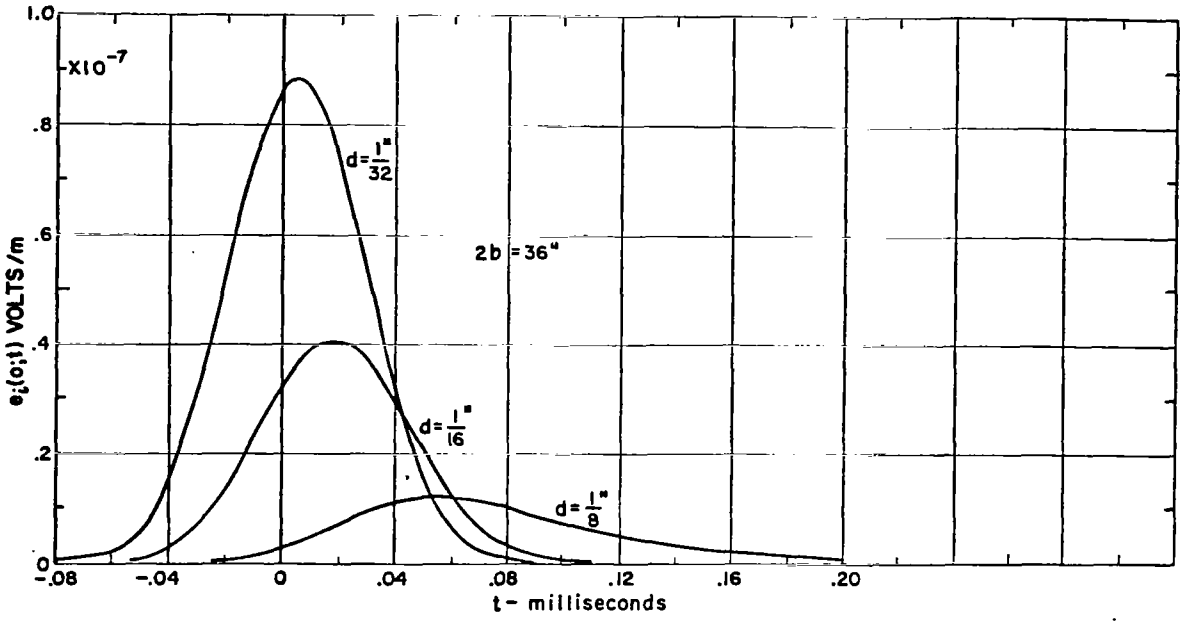

Figure 8c. Dual Plate Shield. $e_o(0)$ = 1 volt/m, t_1 = 24 μs

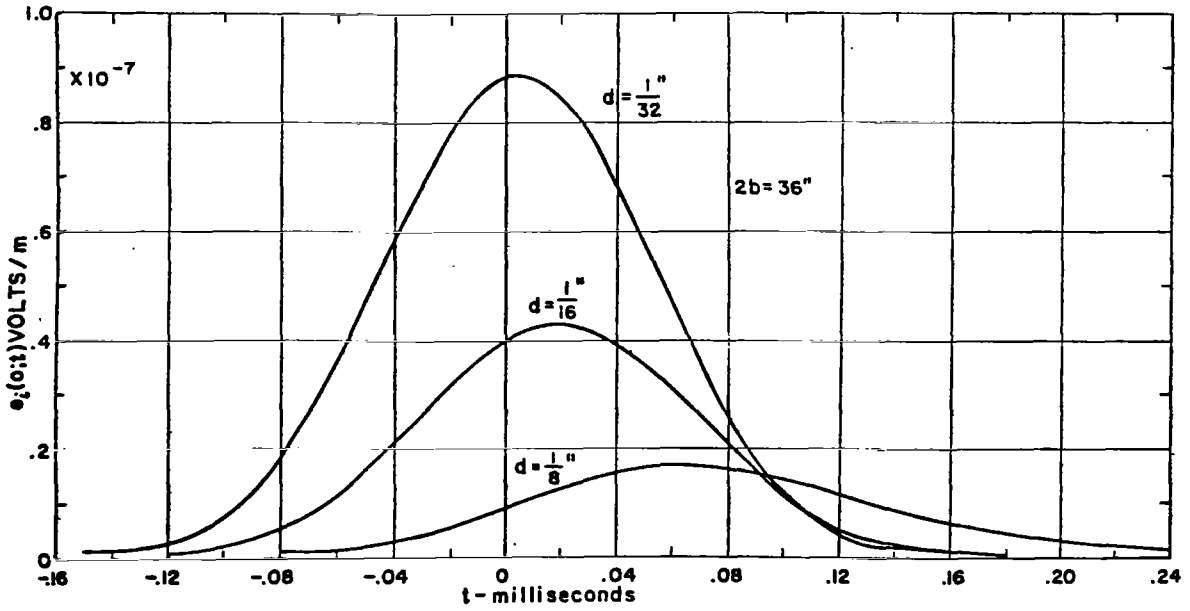

Figure 8d. Dual Plate Shield. $e_o(0)$ = 1 volt/m, t_1 = 48 μs

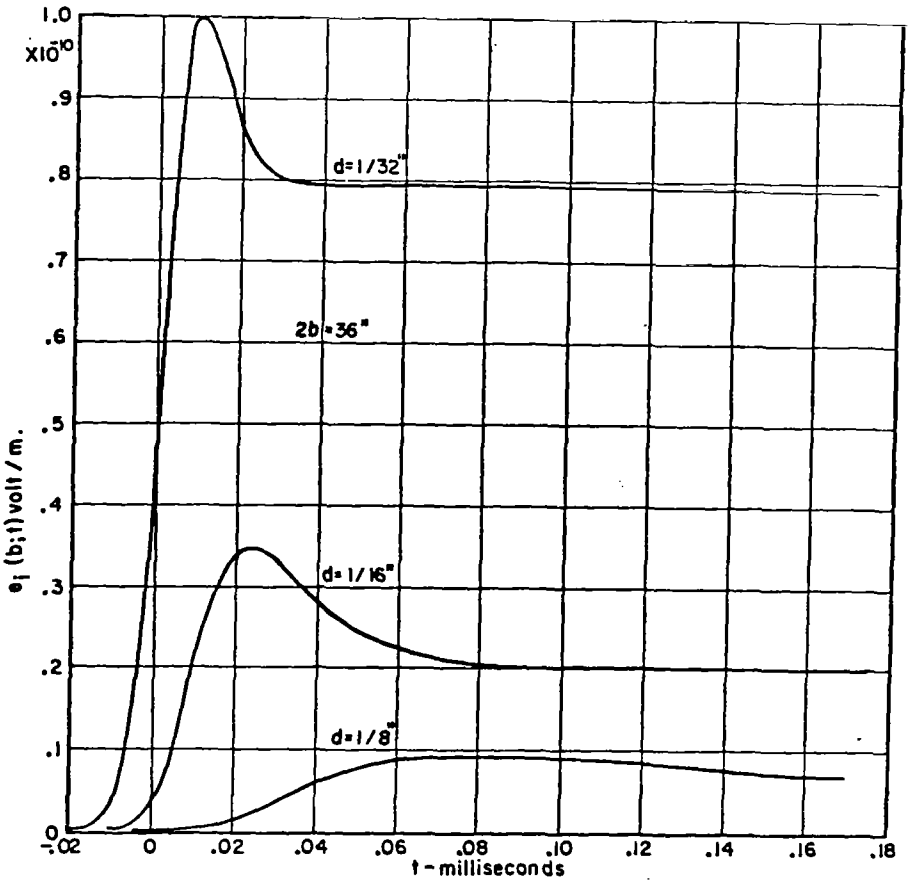

Figure 9a. Dual Plate Shield. $e_o(0)$ = 1 volt/m, t_1 = 6 μs

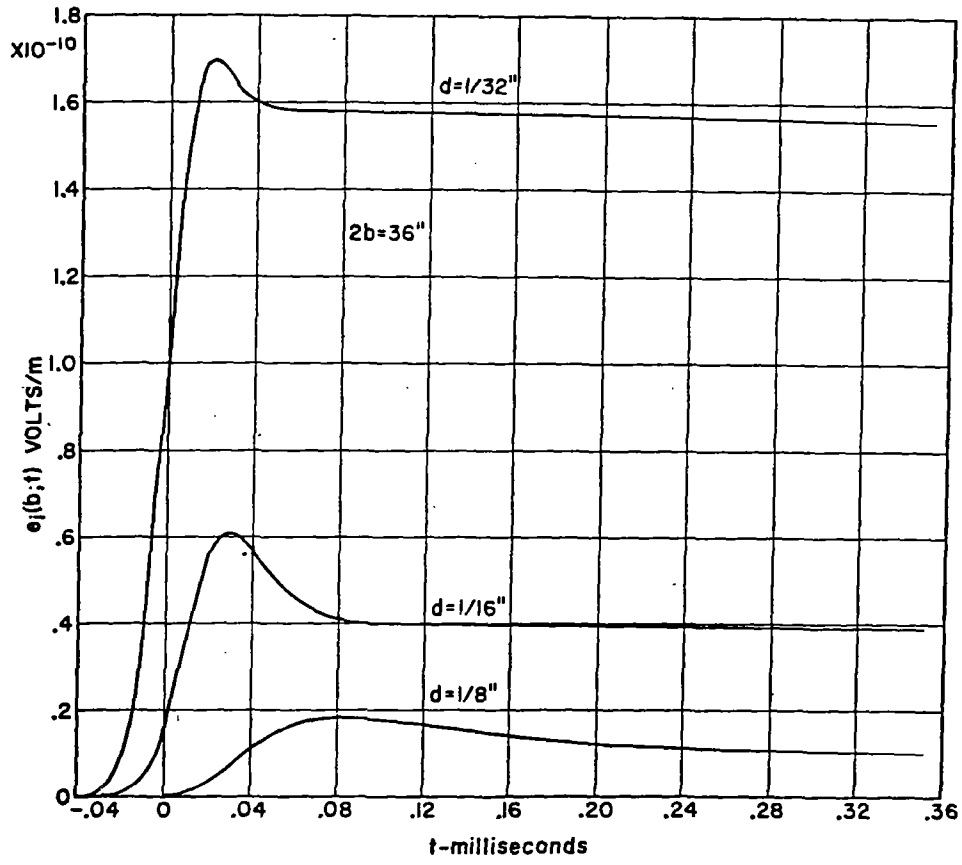

Figure 9b. Dual Plate Shield. $e_o(0)$ = 1 volt/m, t_1 = 12 μs

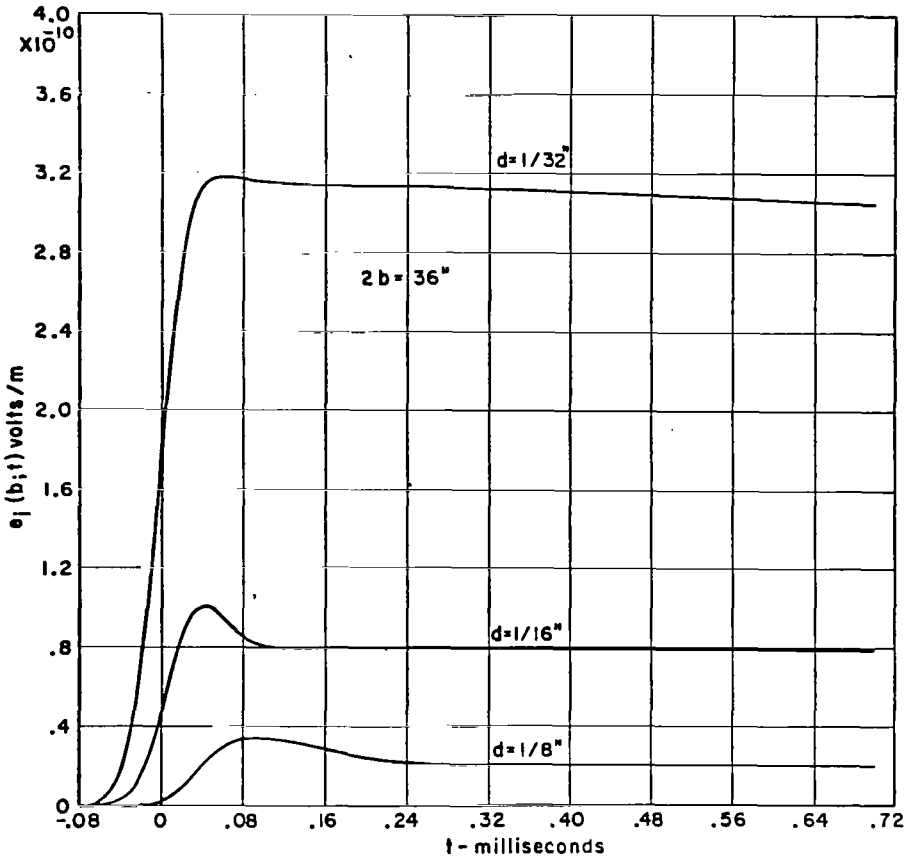

Figure 9c. Dual Plate Shield. $e_o(0)$ = 1 volt/m, t_1 = 24 μs

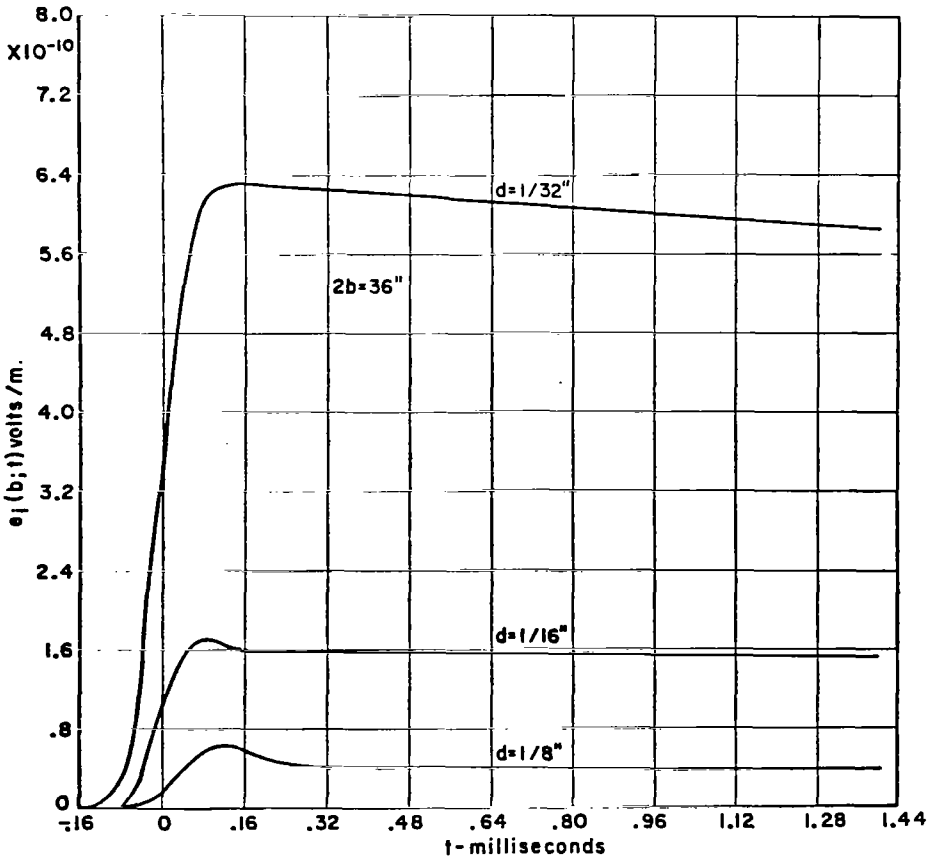

Figure 9d. Dual Plate Shield. $e_o(0)$ = 1 volt/m, t_1 = 48 μs

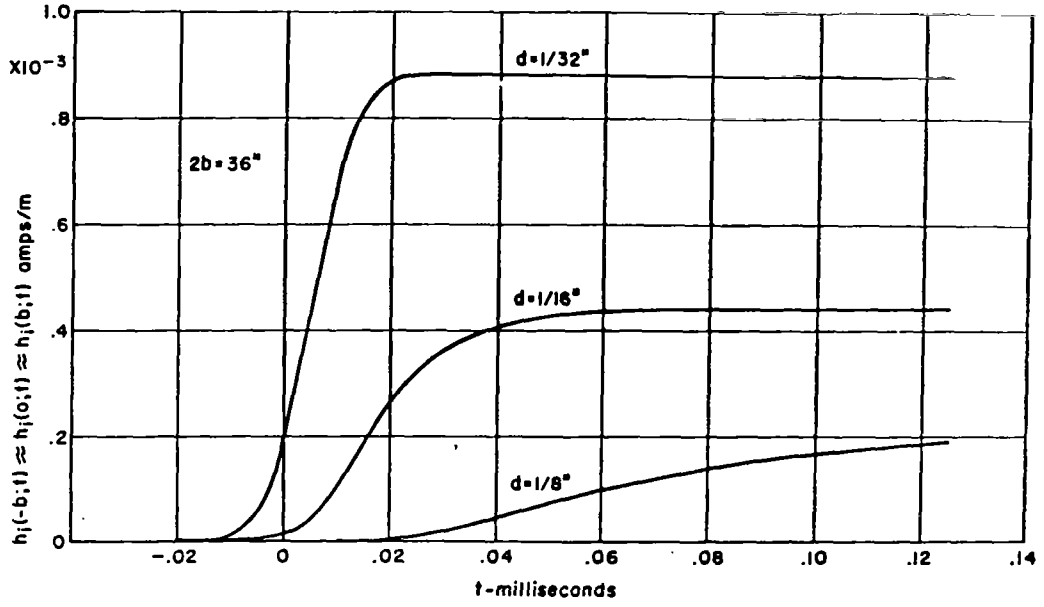

Figure 10a. Dual Plate Shield. $h_o(0) = 1$ amp/m, $t_1 = 6\ \mu s$

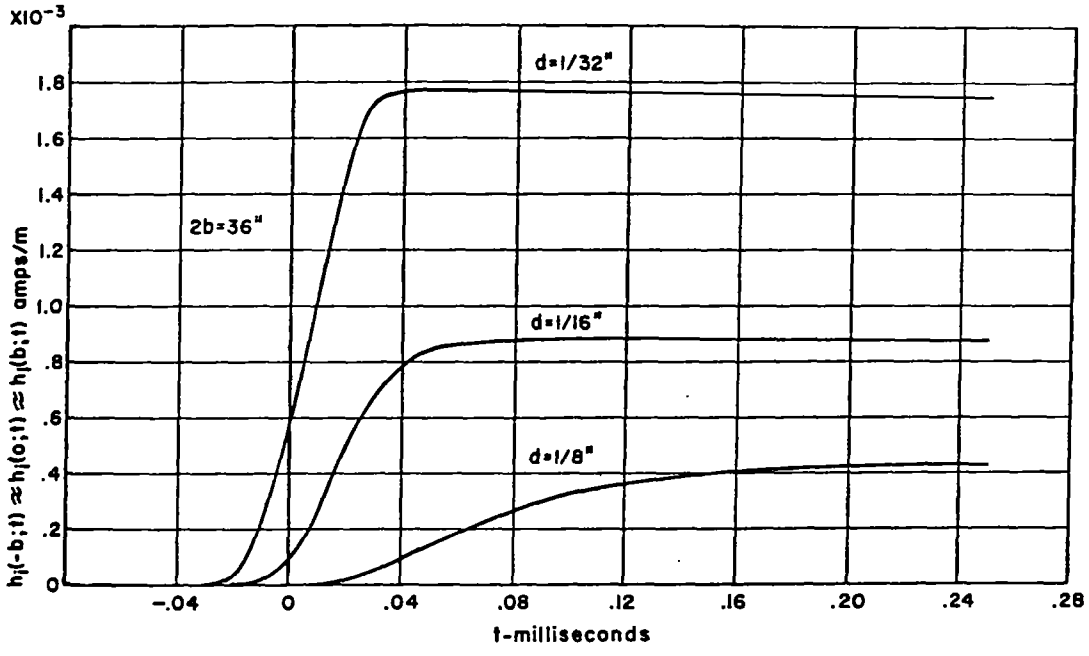

Figure 10b. Dual Plate Shield. $h_o(0) = 1$ amp/m, $t_1 = 12\ \mu s$

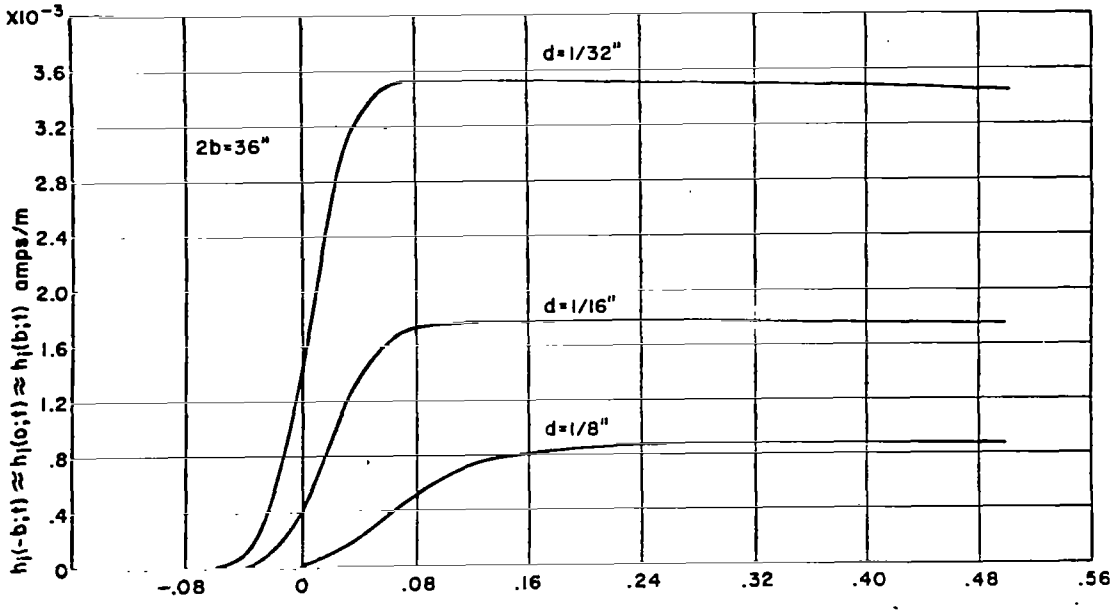

Figure 10c. Dual Plate Shield. $h_o(0) = 1$ amp/m, $t_1 = 24\ \mu s$

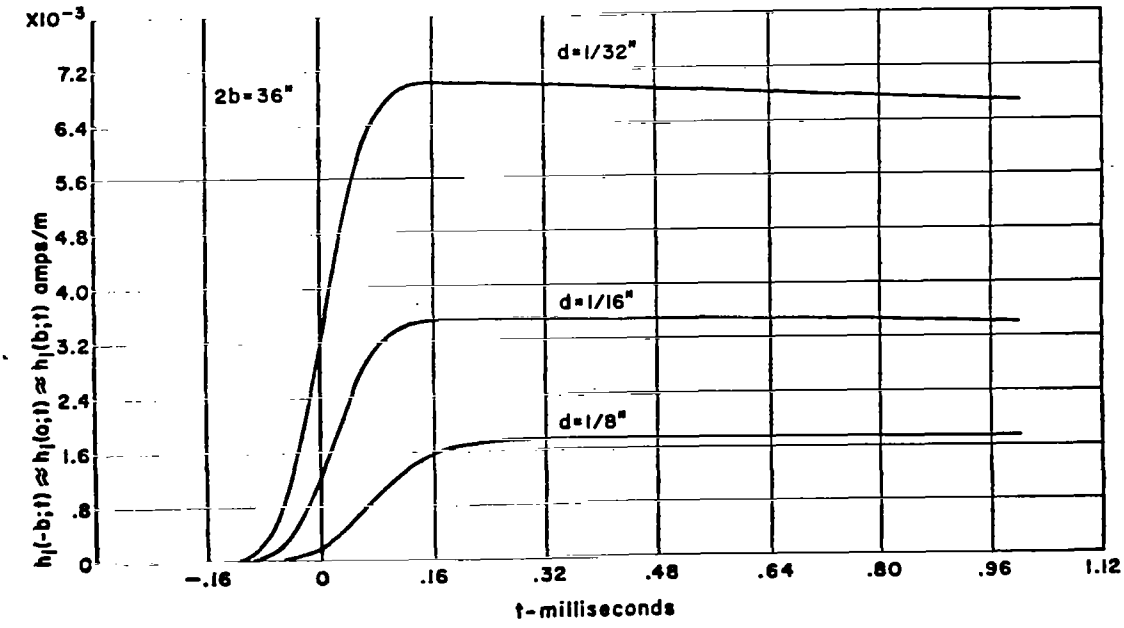

Figure 10d. Dual Plate Shield. $h_o(0) = 1$ amp/m, $t_1 = 48\ \mu s$

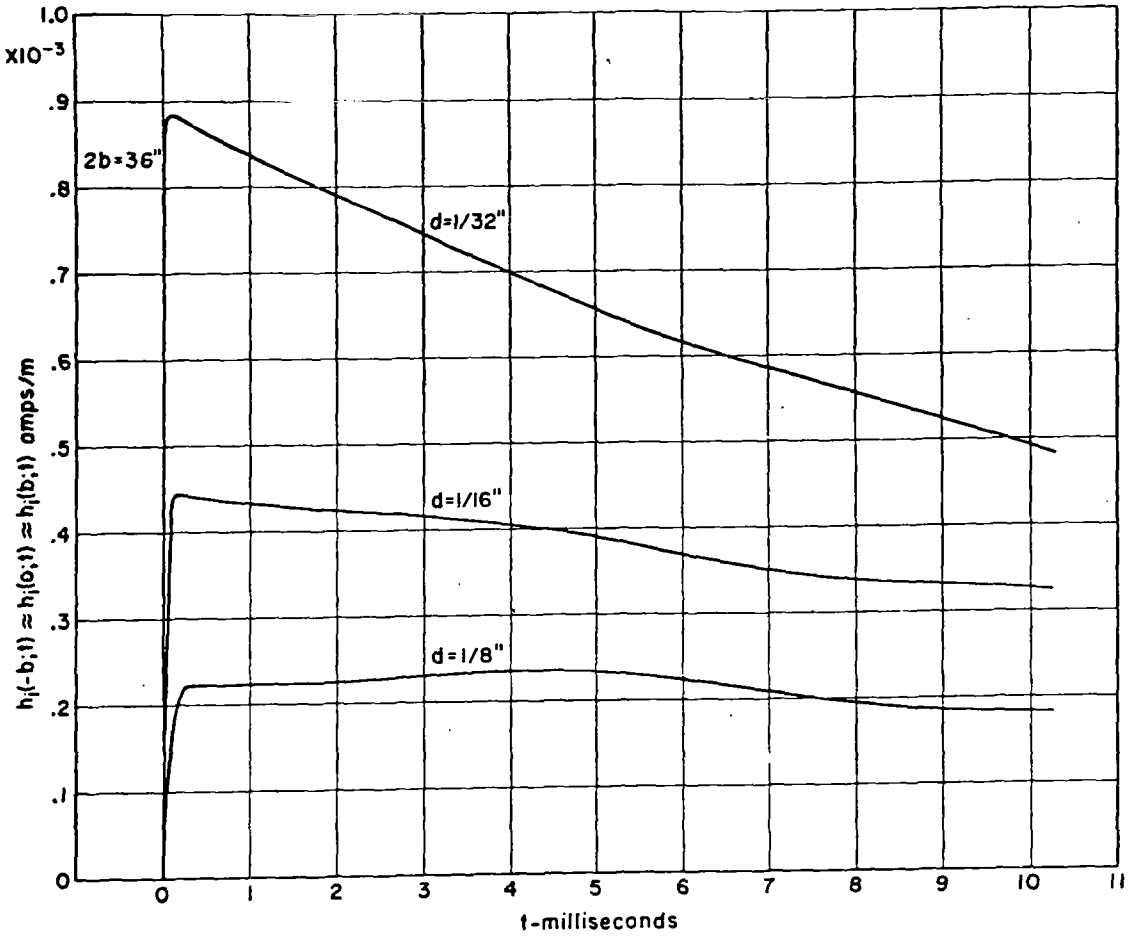

Figure 11a. Dual Plate Shield. $h_o(0)$ = 1 amp/m, t_1 = 6 μs

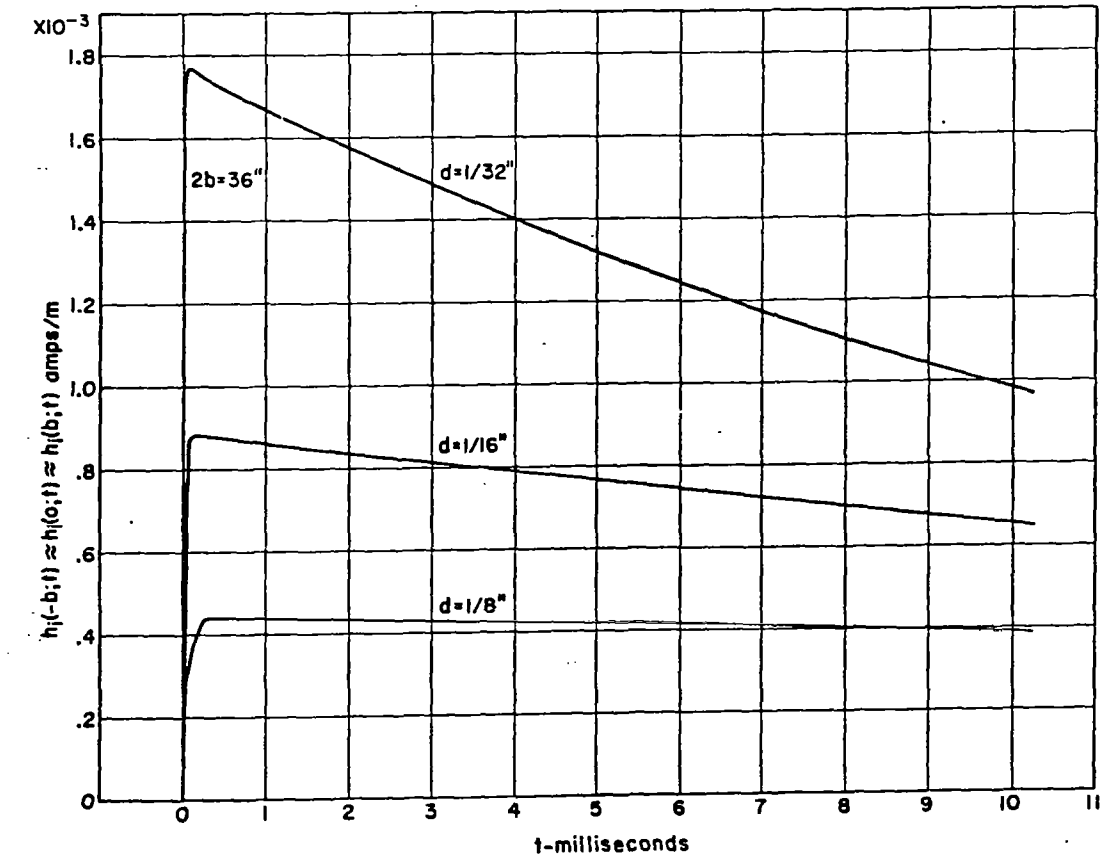

Figure 11b. Dual Plate Shield. $h_o(0)$ = 1 amp/m, t_1 = 12 μs

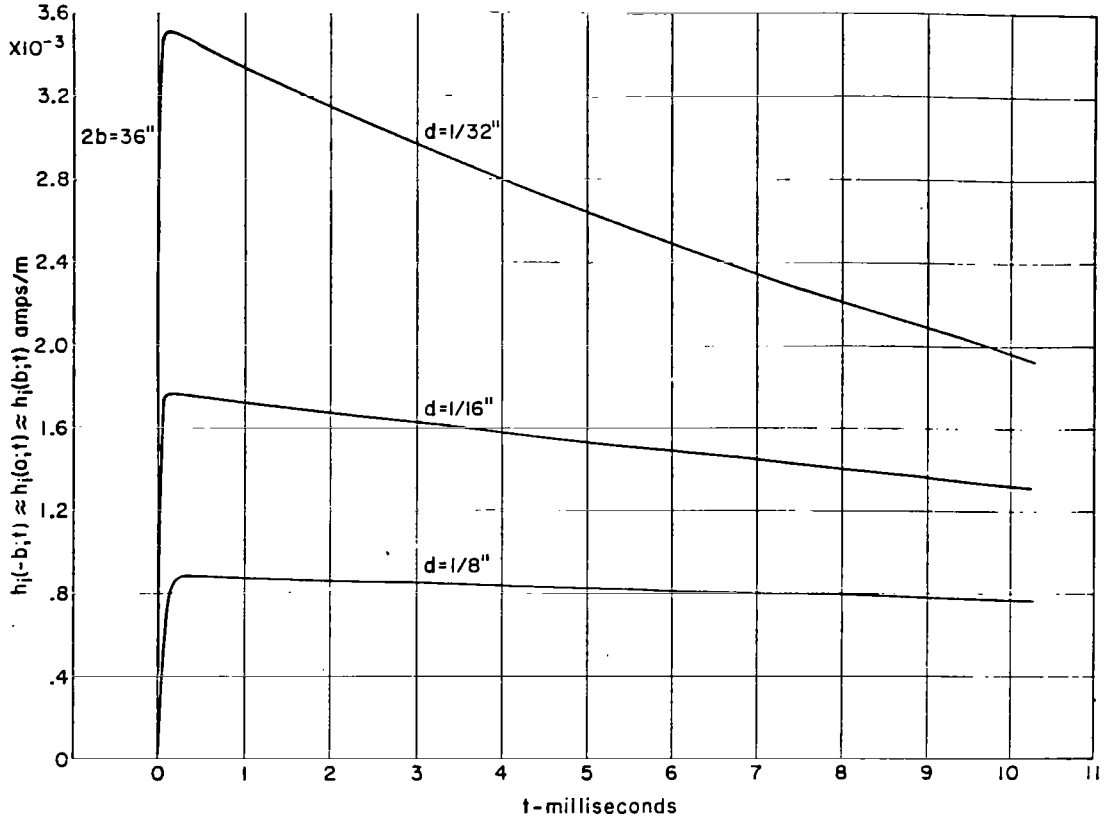

Figure 11c. Dual Plate Shield. $h_o(0)$ = 1 amp/m, t_1 = 24 μs

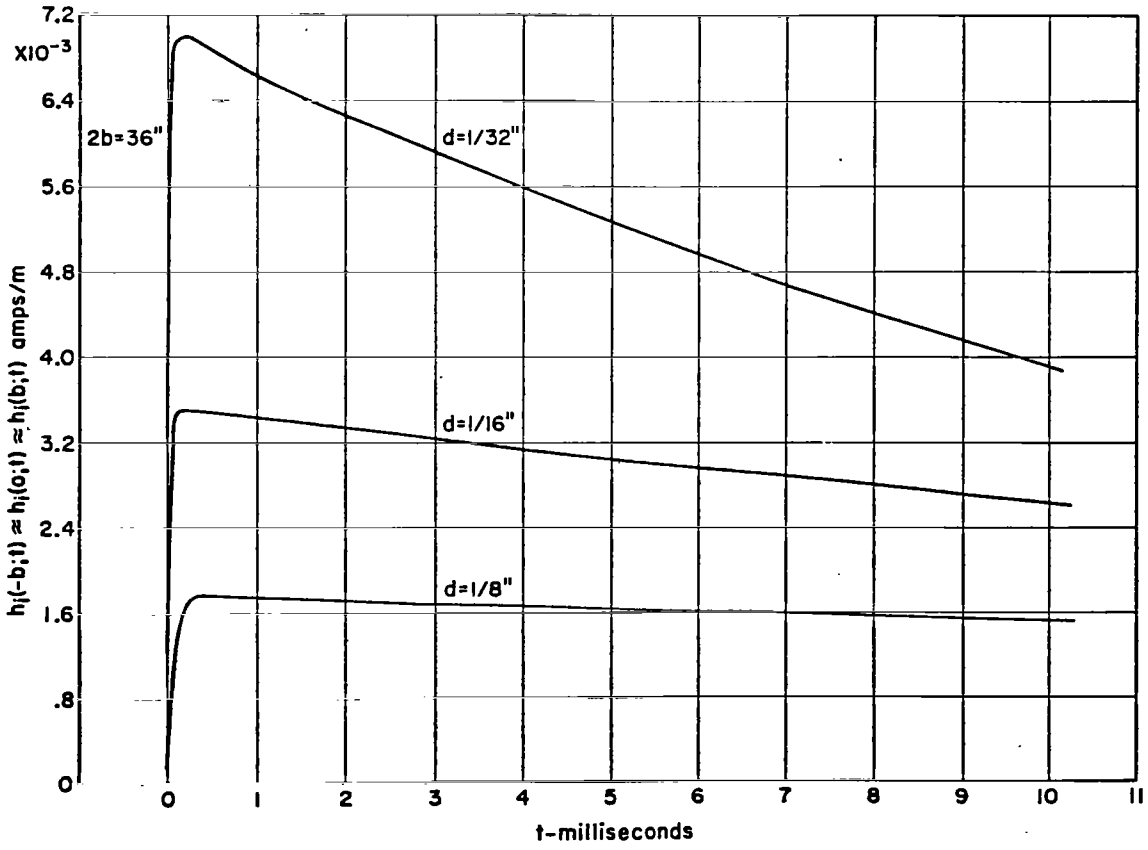

Figure 11d. Dual Plate Shield. $h_o(0)$ = 1 amp/m, t_1 = 48 μs

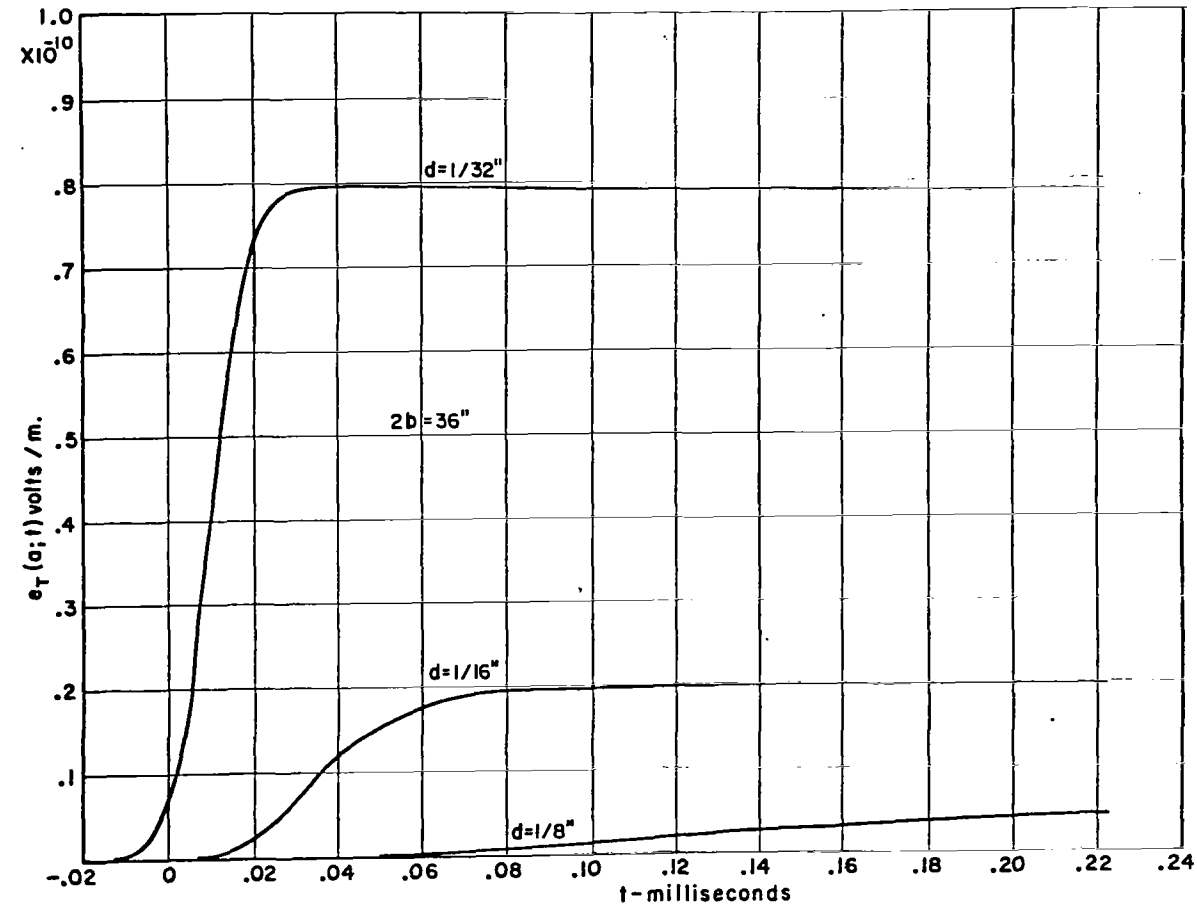

Figure 12a. Dual Plate Shield. $e_o(0)$ = 1 volt/m, t_1 = 6 μs

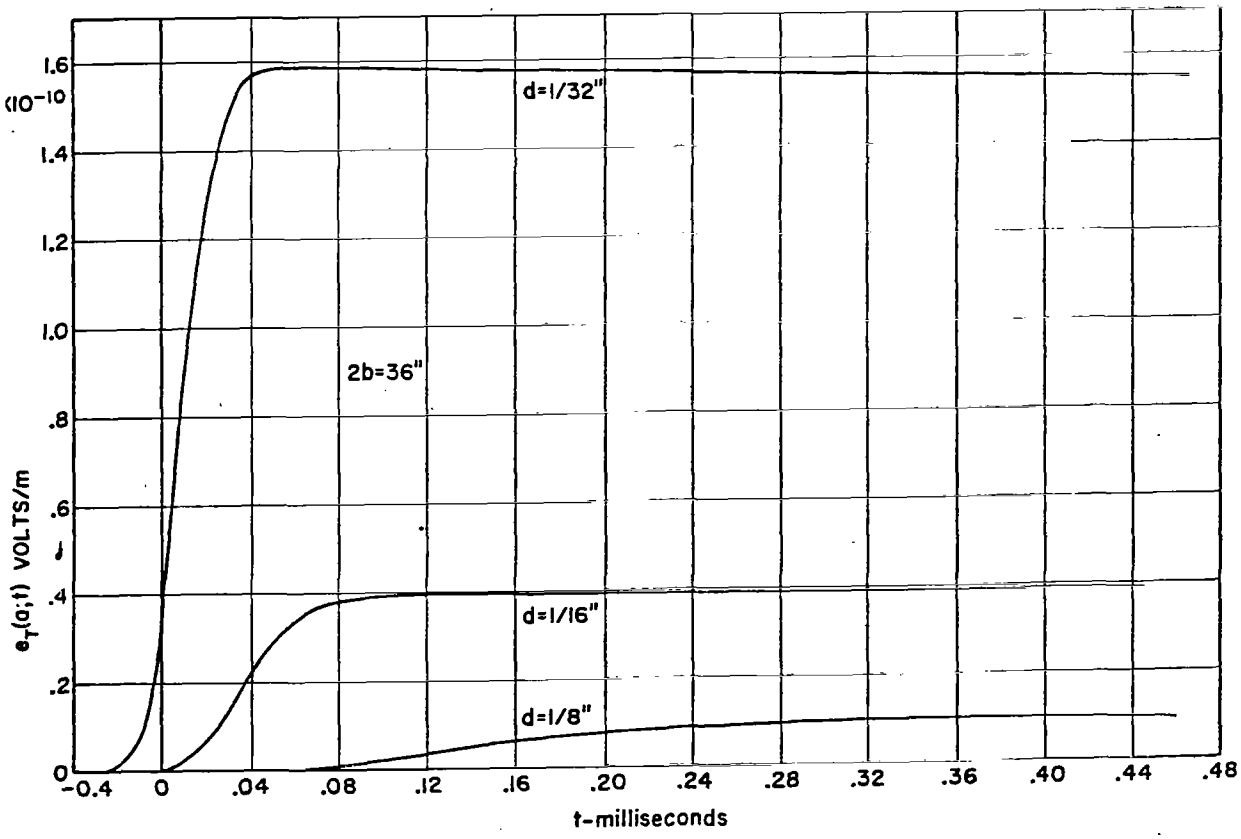

Figure 12b. Dual Plate Shield. $e_o(0)$ = 1 volt/m, t_1 = 12 μs

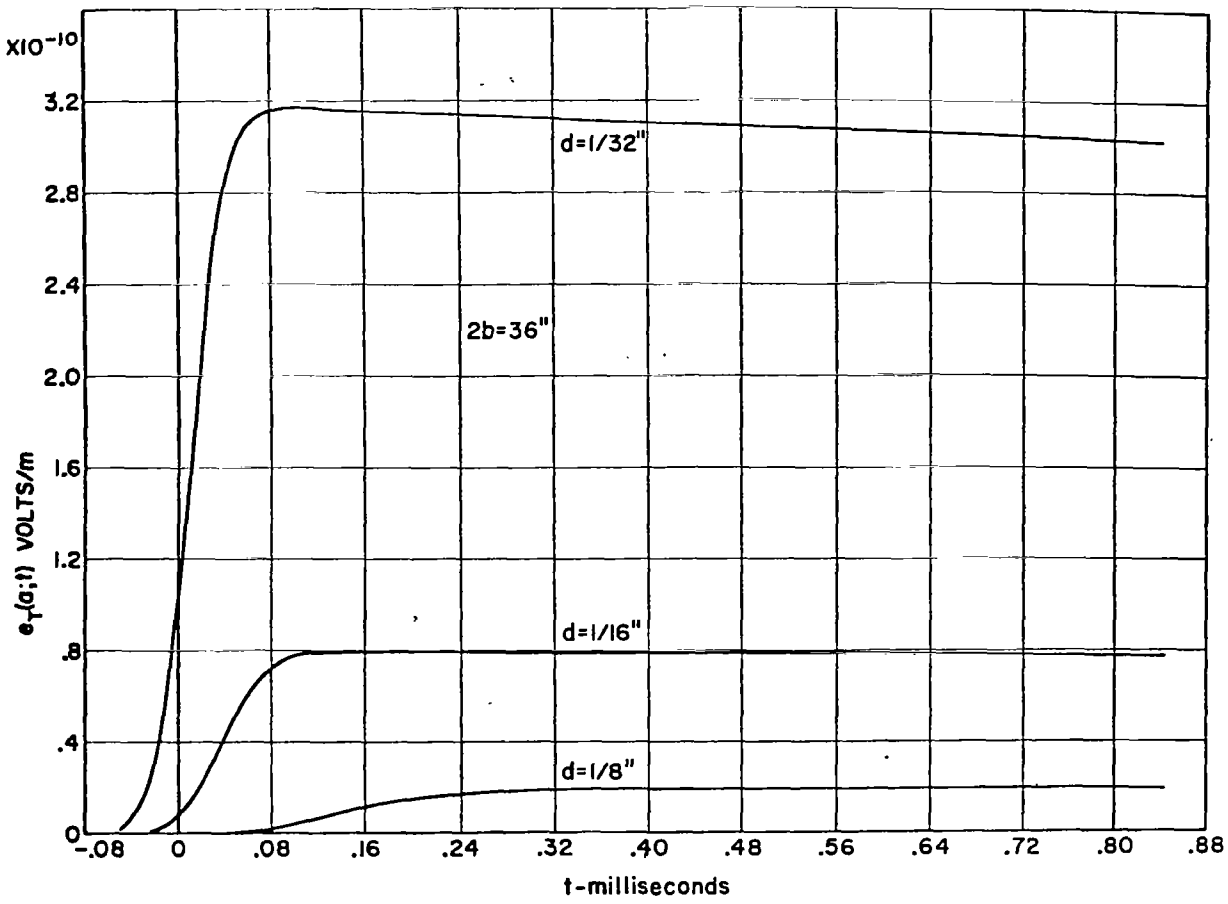

Figure 12c. Dual Plate Shield. $e_o(0) = 1$ volt/m, $t_1 = 24\ \mu s$

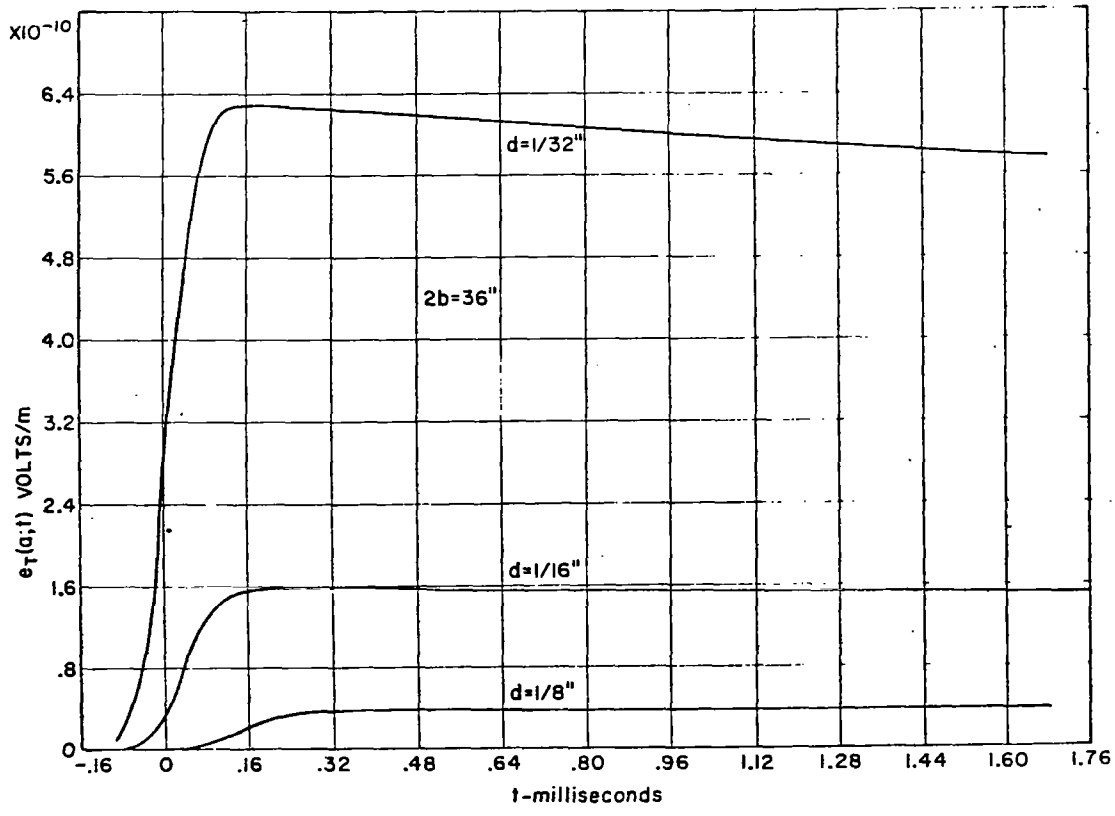

Figure 12d. Dual Plate Shield. $e_o(0) = 1$ volt/m, $t_1 = 48\ \mu s$